Continuity Equation Model of the Predicted Drastic Retreat of Columbia Glacier, Alaska

By L. A. RASMUSSEN *and* M. F. MEIER

STUDIES OF COLUMBIA GLACIER, ALASKA

GEOLOGICAL SURVEY PROFESSIONAL PAPER 1258-A

A discussion of a one-dimensional numerical model developed to predict the retreat and the iceberg discharge from a large iceberg-calving glacier

UNITED STATES GOVERNMENT PRINTING OFFICE, WASHINGTON:1982

UNITED STATES DEPARTMENT OF THE INTERIOR

JAMES G. WATT, *Secretary*

GEOLOGICAL SURVEY

Dallas L. Peck, *Director*

**For sale by the Distribution Branch, U.S. Geological Survey,
604 South Pickett Street, Alexandria, VA 22304**

CONTENTS

	Page
Symbols and abbreviations	AIV
Abstract	1
Introduction	1
Glacier geometry	3
Flux calculations	3
Calving mechanism	4
Columbia Glacier data	6
Longitudinal profiles	A7
Calculated terminus retreat	9
Influence of error in data or model	9
Effect of individual errors	9
Effect of superimposed errors	15
Effect of numerical error	17
Discussion	17
References cited	23

ILLUSTRATIONS

		Page
FIGURE 1.	Index map of Columbia Glacier, Alaska	A2
2.	Surface and bedrock maps of lower reach of Columbia Glacier, Alaska	5
3.	Diagram showing geometry of a typical glacier cross section (at x_i), showing half of the symmetric structure	6
4–22.	Graphs showing:	
4.	Longitudinal geometry of lower reach of Columbia Glacier, Alaska	8
5.	Position of the terminus as a function of time	10
6.	Prime set (case 1) of postulated longitudinal profiles	10
7.	Sensitivity of the model results to the value of the calving coefficient c	11
8.	Features of the calculations for $c = 28.3$	12
9.	Longitudinal profiles assumed by the glacier in the calculations using the case 1 data and $c = 28.3$	14
10.	Volume balance functions, $\dot{b}'(z)$, for cases 1, 2a, 2b, 2c, and 2d	15
11.	Centerline bed altitude profiles, $U(x)$, for cases 1, 4a, and 4b	16
12.	Shoal bathymetry, $U(x)$, for cases 1, 5a, and 5b	17
13.	Longitudinal profiles for case 6a that delay the transition from continuing vigorous thinning to beginning to approach $f_\infty(x)$	18
14.	Longitudinal profiles for case 6b that hasten the transition from continuing vigorous thinning to beginning to approach $f_\infty(x)$	18
15.	Longitudinal profiles for case 7a that are compatible with an initial retreat rate of $\dot{X}_i = -36$ m/a	19
16.	Longitudinal profiles for case 7b that are compatible with an initial retreat rate of $\dot{X}_i = -54$ m/a	19
17.	Final longitudinal profile, $f_\infty(x)$, for cases 1, 8a, 8b, and 8c	20
18.	Effect on the solution of varying the bed topography, $U(x)$	20
19.	Effect on the solution of varying the shoal bathymetry, $U(x)$	21
20.	Effect on the solution of varying the initial retreat rate, $\dot{X}_i$	21
21.	Effect on the solution of varying the final longitudinal profile, $f_\infty(x)$	22
22.	Resultant summation of the individual errors that may be present in the data used to describe Columbia Glacier	22

TABLES

		Page
TABLE 1.	Effect on the calving calculation of varying one or another of the components of the data while holding all others at the values used in the prime case	A13
2.	Effect on the calving calculation of varying one component and simultaneously adjusting c	14
3.	Effect on the solution due to truncation error	17

SYMBOLS AND ABBREVIATIONS

Symbol	Name	Units (where applicable)
A	Glen's flow law parameter	$a^{-1}bar^{-n}$
a	Year.	
α	Glacier surface slope	dimensionless
$\dot{b}$	Local ice balance rate, in ice equivalent	m/a
$\dot{b}'$	Ice balance rate function, in ice equivalent	m/a
c	Calving coefficient related to average water depth	a^{-1}
$\hat{c}$	Calving coefficient related to maximum water depth	a^{-1}
D	Valley cross-section power-law parameter.	
F	Intermediate quantity (eqs. 21, 22)	km/a
$f(x)$	Longitudinal surface profile	km
G	Standard deviation of data error	a
g	Acceleration due to gravity	km/a^2
γ	Shape factor for scaling surface velocity to average velocity through thickness	dimensionless
h	Glacier thickness, in the z direction	km
h_w	Water depth at centerline at terminus	km
$\bar{h}_w$	Average water depth across width at terminus	km
i	Subscript denoting terminus position	dimensionless
j	Subscript denoting x coordinate	dimensionless
k	Subscript denoting upglacier end of lower reach	dimensionless
km	Kilometer.	
M	Measure of error in predicted retreat	dimensionless
m	Meter.	
m	Subscript denoting retreated terminus position	dimensionless
n	Glen's flow law exponent	dimensionless
P	Probability level of data error	dimensionless
Q	Glacier flux	km^3/a
Q_b	Balance flux	km^3/a
Q_c	Calving flux	km^3/a
Q_t	Thinning flux	km^3/a
R	Volume loss above lower reach of glacier	km^3
r	Valley cross-section power-law exponent.	
ρ	Ice density.	
S	Area of glacier cross section	km^2
s	Shape factor	dimensionless
t	Time	a
U	Centerline bed altitude	km
V	Volume of lower reach of glacier	km^3
v	Glacier surface speed, horizontal component	km/a
v_c	Calving speed	km/a
W	Glacier width	km
X	Terminus position	km
$\dot{X}$	Rate of advance of terminus	km/a
X_e	Early estimated retreat	km
X_l	Late estimated retreat	km
x	Horizontal coordinate, positive in direction of flow	km
Z	Glacier surface altitude	km
z	Vertical coordinate, positive upward	km

READEX FICHE best copy available

CONTINUITY EQUATION MODEL OF THE PREDICTED DRASTIC RETREAT OF COLUMBIA GLACIER, ALASKA

By L. A. RASMUSSEN and M. F. MEIER

ABSTRACT

A one-dimensional numerical model based on the continuity equation is developed to predict the retreat rate of the terminus of Columbia Glacier, a large (1,100 km²) grounded iceberg-calving glacier, and to estimate the time distribution of the attendant iceberg discharge. An extensive field program, using September 1, 1977, through August 31, 1978, as the principal data year, obtained ice surface altitudes and velocities, mass-balance values and thickness changes, and bed topography estimated from radio-echo sounding.

For the terminus itself, the continuity equation is used to express the retreat rate as the difference between the glacier flux to the terminus and the iceberg flux from it. The continuity equation also is applied to the lower 14 km of the glacier, which constitutes about 5 percent of its 1978 area, to determine the ice flux to the terminus as the sum of the ice flux into the lower reach of the glacier and the flux increment resulting from the thinning of the lower reach not due to ablation. The iceberg flux is assumed to be proportional to the average water depth at the terminus. The seasonal variations of calving and mass balance are averaged through the year so that all calculations are performed on annualized data.

Instead of independently calculating the glacier flow dynamics, the model requires that a sequence of longitudinal profiles be supplied. On the basis of the calving relation and the other applications of the continuity equation, the model then determines the times at which the glacier assumes each of the supplied profiles. The effect on the predicted retreat rate caused by the arbitrariness of the longitudinal profiles used to describe the lower reach of Columbia Glacier appears to be less than the effect of other uncertainties in the data used.

The predicted retreat slowly accelerates from the initial observed rate of 45 m/a until 1983.0±0.9, when the terminus reaches deep water, and the retreat rate rapidly increases to about 4 km/a. By some time between 1983.8 and 1986.5, the terminus is expected to have retreated 9.5 km. A maximum iceberg calving flux of about 10 km³/a, which is 6 to 8 times the initial amount, is expected to occur in about 1983. It is assumed, in making this prediction, that the annual mass balance and other factors do not substantially differ from the 1977–78 observation.

INTRODUCTION

Nearly all grounded, iceberg-calving glaciers experience large-scale asynchronous advances and retreats. This behavior apparently is not directly related to climatic variations. A critical factor is the water depth at the terminus, as instability results when the glacier retreats even a short distance into a deep fiord or basin. The glacier then may retreat rapidly and irreversibly as unusual volumes of ice break away (Post, 1975). Observations of such glaciers reveal that they can advance only by moving a moraine shoal forward, so that the terminus rests in shallow water.

Columbia Glacier, near Valdez, Alaska (fig. 1), is a large calving glacier; it is 67 km long and 1,100 km² in area. It ends on a moraine shoal in shallow water, but, upglacier from the terminus, the bed is about 400 m below sea level. Except for some small areas associated with ice-dammed lakes, the glacier is grounded throughout; none of it is floating at the terminus. Although the position of the terminus has been in a state of near equilibrium since the first recorded observation in 1794, evidence now suggests that rapid, drastic retreat may be imminent (Post, 1975). Small icebergs drift from Columbia Glacier toward and occasionally into Valdez Arm (Kollmeyer and others, 1977). Drastic retreat would substantially increase the discharge of ice and, thus, would increase the iceberg hazard to shipping. To determine when this might happen and how much the iceberg discharge might increase, the U.S. Geological Survey began an intensive study in 1977 (Meier and others, 1978). Much of the field data has been reported (Mayo and others, 1979), and a preliminary prediction was issued in 1980 (Meier and others, 1980).

This report describes a newly developed time-dependent, one-dimensional numerical model, based mainly on an equation of continuity that can be used to calculate the terminus retreat and the rate of iceberg discharge for a calving glacier. This simple model was developed and used for the Columbia Glacier prediction because more complex models, which fully utilized glacier dynamics theory, could not be developed by the time the prediction had to be given. The simple model described here has been tested on one other calving glacier and should have general application to the study of the asynchronous variations and the rapid retreats of other calving glaciers. Because the model does not include inde-

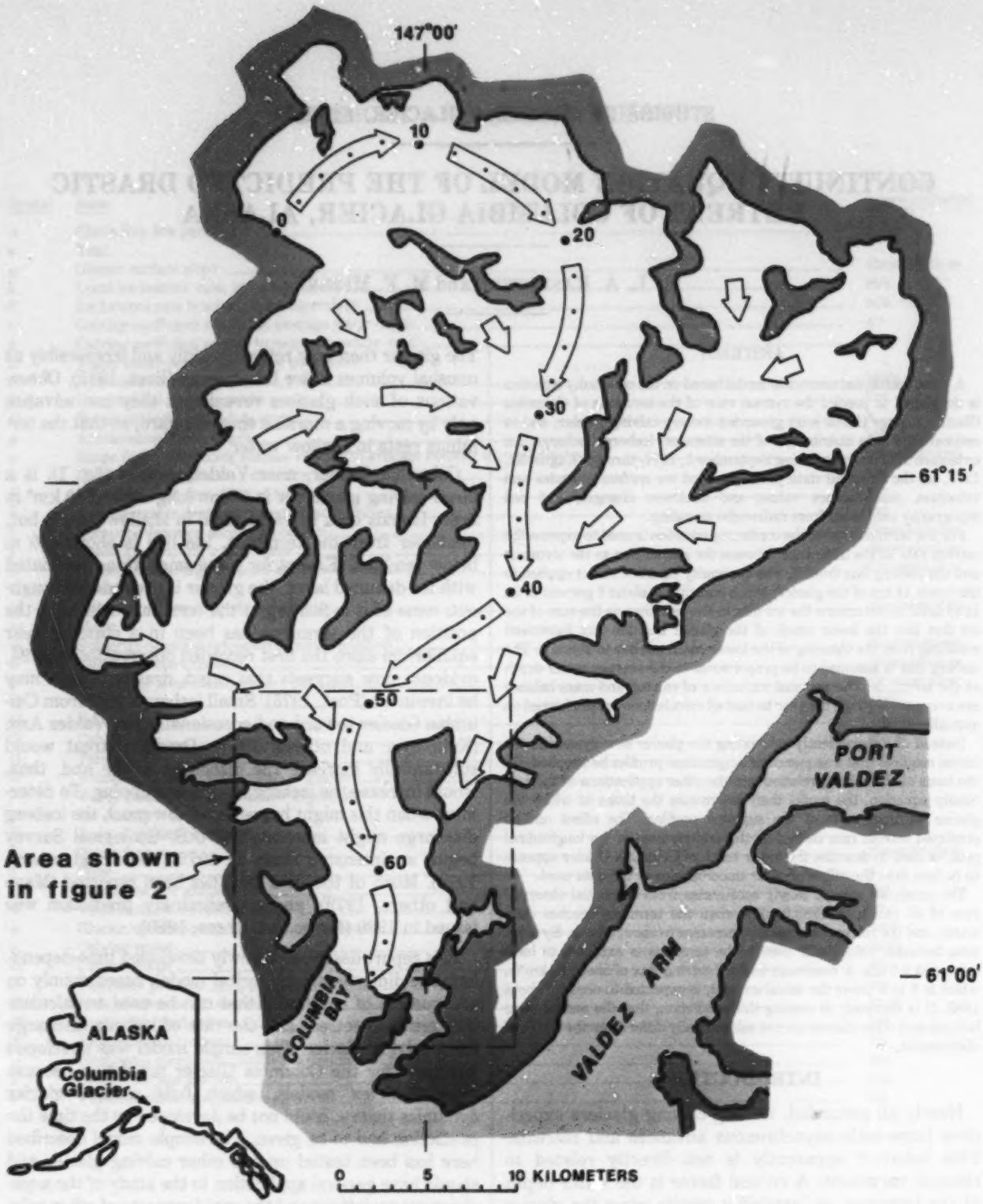

FIGURE 1.–Index map of Columbia Glacier, Alaska. Arrows show direction of flow. Main ice stream is indicated by longer arrows and dots at 2-km intervals along the longitudinal coordinate system.

pendent calculation of the glacier flow dynamics, it can be applied only to a glacier that, on an annual basis, is already retreating.

The report begins with a description of how the three-dimensional shape of the lower Columbia Glacier is described in terms of one independent space dimension, by using a simple analytic approximation of the cross-sectional shape (see section entitled "Glacier Geometry"). The ice flux (discharge), consisting of time- and distance-varying combinations of balance flux and thinning flux components, is examined in the section "Flux Calculations." A terminus boundary condition, a relation between calving speed and water depth, is discussed in "Calving Mechanism."

The one-dimensional numerical model requires that the field data, obtained over three-dimensional space, be averaged, smoothed, or otherwise transformed to form a one-dimensional data set; this is described in the section "Columbia Glacier Data." A crucial aspect of this model is the need for future longitudinal surface profiles. The section entitled "Longitudinal Profiles" explains how these profiles are constructed. The profiles are not initially identified with time; the model calculates when the glacier reaches each profile and, thus, predicts the time-variation of terminus retreat and the iceberg flux (see "Calculated Terminus Retreat").

The section entitled "Influence of Error in Data or Model" describes the influence of error in the data or in the assumptions of the model on the calculated terminus retreat and iceberg flux and includes the effect of numerical error. The results of this sensitivity analysis are summarized in a set of tables. Finally, the quality of the prediction and its sensitivity to data error and model assumption are examined and discussed in the last section (see "Discussion").

GLACIER GEOMETRY

The lower reach of the glacier is represented by a longitudinal coordinate system (x,z) in which x is the horizontal slightly curvilinear axis (fig. 2), positive in the direction of flow, and z is the vertical axis, positive upward. The terminus position is denoted X, and the altitude of the glacier surface, Z. Data are provided at a set of x_i that are equally spaced and numbered in the direction of negative x (during retreat this is the direction X changes with time), so that $x_{i+1}=x_i-\Delta x$ and

x_1 is the position of the terminus X at time t_1,
x_m is the position of the terminus X at time t_m, and
x_k is the farthest point considered up the glacier.

When the terminus position $X=x_i$ at time t_i, the longitudinal surface profile is denoted $f_i(x)$, which is the piecewise linear function defined by the points (x_i,Z_{ii}), (x_{i+1},Z_{i+1}), . . . , (x_k,Z_{ik}). That is, $X_{ij}=f_i(x_j)$. In general, where a variable has two subscripts, the second refers to the x location of the value, and the first refers to the x location of the terminus. Thus, where θ is any variable, θ_{ij} is the value of θ at x_j when the terminus is at x_i.

The valley cross section is assumed to follow a power law; that is, the width at altitude z is

$$W(z)=D(z-U)^r \tag{1}$$

where U is the bed altitude at the valley centerline and the power law parameters are D and r. The area of the cross section is obtained by integrating the width

$$S(z)=\int_U^z W(z)dz=D(z-U)^{r+1}/(r+1)=W(z)h(z)/(r+1) \tag{2}$$

in which a horizontal transverse glacier surface profile is assumed and where

$$h(z)=z-U \tag{3}$$

is the glacier thickness at the centerline (fig. 3). If, for some z, the width, area, and centerline depth are specified, then the power law parameters are obtained:

$$\left.\begin{aligned} r&=W(z)h(z)/S(z)-1\\ D&=W(z)/h^r(z). \end{aligned}\right\} \tag{4}$$

For a concave cross section, $0<r<1$, and thus

$$1<W(z)h(z)/S(z)<2. \tag{5}$$

If the bed at the centerline is below sea level ($U<0$), then the centerline water depth is $\bar{h}_0=-U$, and the average water depth across the width of the glacier is

$$\bar{h}_0=S(0)/W(0)=h_0/(r+1)=-U/(r+1). \tag{6}$$

Water depth is defined as the vertical distance below sea level to the bed; it is taken to be positive.

The geometry of the lower reach of the glacier is determined by specifying the initial longitudinal profile, $f_1(x)$, and, for $1\le j\le k$, the valley centerline altitudes, U_j, and the initial cross section widths, W_{1j}, and areas, S_{1j}. From these, the power law parameters D_j and r_j are found by using equations 3 and 4. For any other longitudinal profile, $f_i(x)$, equations 1 and 2 are used for $i\le j\le k$ to get the corresponding widths, W_{ij}, and areas, S_{ij}.

FLUX CALCULATIONS

As the terminus recedes from $X=x_i$ at time t_i to $X=x_{i+1}$ at time t_{i+1}, the cross-section area change at any $x_k\le x_j\le x_i$ is

$$(\Delta S_j)_i=S_{i+1,j}-S_{ij}, \tag{7}$$

and the total volume change over the entire lower reach is calculated, by integrating trapezoidally,

$$V_{i+1/2}=\frac{1}{2}\sum_{j=i}^{k-1}(x_j-x_{j+1})[(\Delta S_j)_i+(\Delta S_{j+1})_i] \quad (8)$$

where $(\Delta S_k)_i$ is defined to be zero. This volume change contributes a flux component at the terminus:

$$(\Delta Q_s)_{i+1/2}=\frac{-\Delta V_{i+1/2}}{t_{i+1}-t_i} \quad (9)$$

The volume $\frac{1}{2}(x_i-x_{i+1})(S_{ii}+S_{i+1,i+1})$ is lost to calving (see equation 18). When the terminus is at $X=x_i$, the balance over the lower reach also contributes a flux component at the terminus

$$(\Delta Q_s)_i=\frac{1}{2}\sum_{j=1}^{k-1}(x_j-x_{j+1})[W_j\dot{b}(Z_{ij})+W_{j+1}\dot{b}(Z_{i,j+1})] \quad (10)$$

where $\dot{b}(Z)$ is a balance function, in ice equivalent.

The total flux at x_k, the top of the lower reach, is assumed to obey Glen's flow law (Glen, 1954), and the flow is assumed to be laminar (longitudinal stresses are neglected). Also, both the deformational and the sliding components of velocity (as in Budd and others, 1979) are taken to follow the same form

$$v=\frac{2Ah}{n+1}(s\rho gh\sin\alpha)^n \quad (11)$$

in which v is the horizontal component of the total velocity at the surface, A and n are the flow law parameters, s is a shape factor, ρ is the density of glacier ice, g is the acceleration due to gravity, and $\tan\alpha=-dZ/dx$ is the surface slope. This equation is not strictly correct because h should be measured perpendicular to the glacier surface. However, the surface slope of the lower Columbia Glacier is rather small ($0.002<\tan\alpha<0.005$); as a result, whether h is measured vertically or perpendicular to the surface makes little difference (Budd and Jenssen, 1975). The total flux through the cross section of area S is then

$$Q=\gamma vS \quad (12)$$

where γ is a shape factor that scales down the surface velocity to give the average velocity through the section (Nye, 1952; Bindschadler, 1978). If, at the top of the lower reach, x_k, equations 2 and 3 are used to express S_{ik} and h_{ik} in terms of Z_{ik}, then equations 11 and 12 can be combined and divided to eliminate A, s, and γ, yielding

$$Q_{ik}/Q_{1k}=[(Z_{ik}-U_k)/(Z_{1k}-U_k)]^{n+2}(\sin\alpha_{ik}/\sin\alpha_{1k})^n \quad (13)$$

where $\sin\alpha_{ik}=\tan\alpha_{ik}/(1+\tan^2\alpha_{ik})^{1/2}$ and $\tan\alpha_{ik}\approx(Z_{ik}-Z_{i,k-1})/\Delta x$, the Z_{ik} being taken from the supplied longitudinal profiles $f_i(x)$. Dividing out A, s, and γ is done on the assumption that the flow characteristics at x_k do not change during the time the terminus retreats from x_1 to x_m.

The total flux to the terminus consists of three components: the flux into the lower reach, the flux contribution caused by thinning of the lower reach, and the flux contribution due to the ice balance at the surface of the lower reach. The average value, as the terminus recedes from x_i to x_{i+1}, of the total flux to the terminus is obtained as the sum of the three components, using equations 9, 10, and 13:

$$Q_{i+1/2}=\frac{1}{2}(Q_{ik}+Q_{i+1,k})+\frac{1}{2}[(\Delta Q_s)_i+(\Delta Q_s)_{i+1}]+(\Delta Q_s)_{i+1/2}. \quad (14)$$

The total flux, Q_{ik}, at the top of the lower reach, x_k, can also be determined by applying the continuity equation to the upper reach of the glacier ($0\le x\le x_k$) in the form

$$Q_{ik}=\int\int(\dot{b}-\dot{h})=\int\dot{b}+\int-\dot{h}=(Q_s)_{ik}+(Q_h)_{ik} \quad (15)$$

where $\dot{b}$ is the local ice balance and $\dot{h}$ is the local glacier thickness change, both averaged annually, and the domain of the integrals is the entire area of the glacier above x_k. At time t_i, the total flux at x_k consists of a balance component $(Q_s)_{ik}$ and a thinning component $(Q_h)_{ik}$.

If the times, t_i, when the terminus positions are at the x_i are known for $1\le i\le m$ and if it is assumed that $(Q_s)_{ik}=(Q_s)_{1k}$ is constant in time, then the total volume removed from the reservoir of ice above x_k (R) may be calculated

$$R=\int_{t_1}^{t_m}(Q_s)_{ik}dt=\int_{t_1}^{t_m}Q_{ik}dt-(t_m-t_1)(Q_s)_{1k} \quad (16)$$

where the time integral is approximately

$$\int_{t_1}^{t_m}Q_{ik}dt=\frac{1}{2}\sum_{i=1}^{m-1}(t_{i+1}-t_i)(Q_{ik}+Q_{i+1,k}), \quad (17)$$

equation 13 being used to compute the Q_{ik}. The determination of R is not necessary to calculating the retreat rate but is useful in estimating the effect the retreat of the terminus has on the remaining glacier.

CALVING MECHANISM

As developed in Meier and others (1980), a calving equation may be obtained by applying the continuity equation at the glacier terminus in the form

$$S\dot{X}=Q-Q_c, \quad (18)$$

FIGURE 2.—Surface and bedrock maps of lower reach of Columbia Glacier, Alaska. Contour interval is 200 m on exposed bedrock, 100 m on glacier surface, and 100 m (dashed) on subglacial terrain. Subglacial terrain map was derived by 2-dimensional continuity adjustment (Sikonia and others, written commun., 1981) from radio-echo sounding and other field measurements. For location, see figure 1.

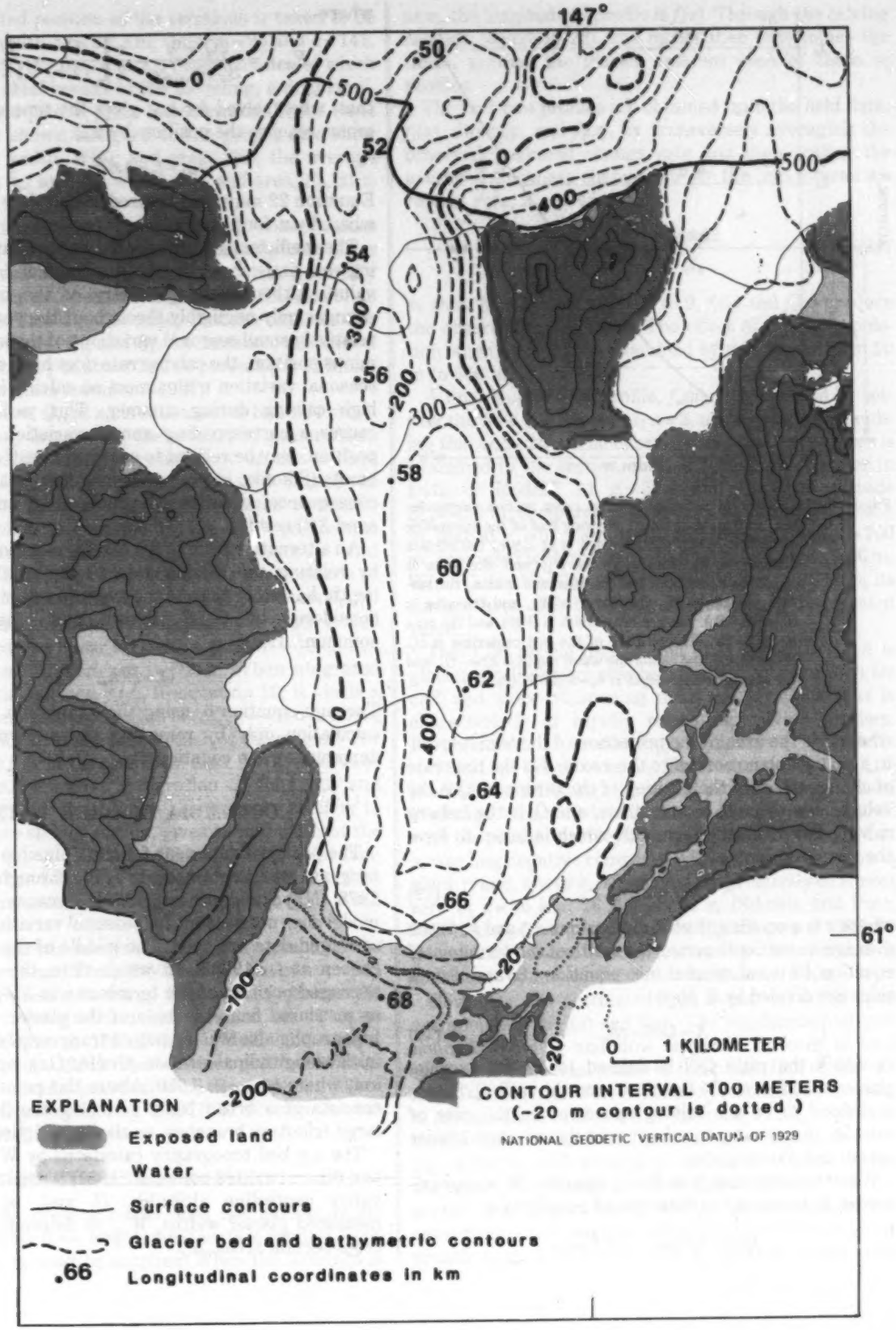
147°
61°
.50
.52
.54
.56
.58
.60
.62
.64
.66
.68
0
500
-400
-300
-200
300
-100
-20
0 1 KILOMETER
CONTOUR INTERVAL 100 METERS
(-20 m contour is dotted)
NATIONAL GEODETIC VERTICAL DATUM OF 1929
EXPLANATION
Exposed land
Water
Surface contours
Glacier bed and bathymetric contours
.66 Longitudinal coordinates in km

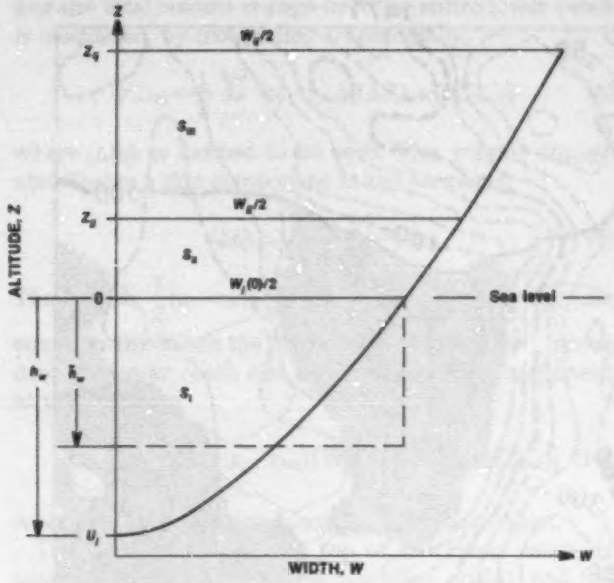

FIGURE 3.—Geometry of a typical glacier cross section perpendicular to the x axis (at x_i), showing half of the symmetric structure. When the terminus is at $x_i > x_{II}$, the surface altitude is Z_0, the width is W_0, and the area is $S_0 = 2(S_I + S_{II} + S_{III})$. When the terminus is at x_{II}, the surface altitude is Z_{II}, the width is W_{II}, and the area is $S_{II} = 2(S_I + S_{II})$. The sea-level width is $W_I(0)$, and the area is $S_I(0) = 2S_I$. The altitude of the bed centerline is U_I. When $U_I < 0$, the centerline water depth is $h_w = -U_I$, and the average water depth is $\bar{h}_w = S_I(0)/W_I(0)$.

where S is the area of the projection of the terminus onto a vertical plane normal to the x axis, $\dot{X}$ is the time rate of change dX/dt of the position of the terminus, Q is the volume flux of ice to the terminus, and Q_c is the iceberg calving flux from the terminus, which is taken to have the form

$$Q_c = Sc\bar{h}_w \tag{19}$$

where c is a coefficient with dimensions a^{-1} and $\bar{h}_w$ is the average water depth across the width of the terminus. If equation 19 is substituted into equation 18, and if both sides are divided by S, then

$$\dot{X} = Q/S - c\bar{h}_w, \tag{20}$$

in which the ratio Q/S is defined to be the average glacier speed, v, at the terminus, and the ratio $Q_c/S = c\bar{h}_w$ is defined to be the calving speed, v_c. In the case of retreat, the calving speed exceeds the average glacier speed, and $\dot{X}$ is negative.

When the terminus is at $X = x_i$, equation 20 is approximated, in terms of the data spaced equally in x,

$$(x_{i+1} - x_i)/(t_{i+1} - t_i) = F_{i+1/2},$$

where (21)

$$F_{i+1/2} = \frac{2Q_i + \frac{1}{2}}{S_{ii} + S_{i+1,i+1}} - \frac{c}{2}\left[\frac{U_i}{1+r_i} + \frac{U_{i+1}}{1+r_{i+1}}\right]$$

that, when solved for t_{i+1}, gives the time when the terminus reaches the position $X = x_{i+1}$:

$$t_{i+1} = t_i - \Delta x/F_{i+1/2}. \tag{22}$$

Equation 22 may then be used to calculate the times, t_i, when $X = x_i$ for $1 \le i \le m$.

The coefficient c gives only the annually averaged calving rate and cannot be used to obtain an instantaneous value. Although the geometry of the entire glacier changes only negligibly throughout the year because of relatively small seasonal variations of thickness and terminus position, the calving rate does have a pronounced seasonal variation with almost no calving in winter and high calving during summer. This variation, which causes a corresponding annual variation in terminus position, may be related to seasonal runoff and lake outbursts (Sikonia, in press; Sikonia and Post, 1980). As a consequence, equation 21 produces an annually averaged $X(t)$ result.

An alternative form of the calving equation is obtained by relating the calving rate to the maximum water depth, h_w, rather than to the average water depth, $\bar{h}_w$, as considered by C. S. Brown and others (written commun., 1980),

$$Q_c = Sch_w. \tag{23}$$

Through equation 6, using the h_w relation modifies the calculation only by removing the r_i terms from the denominators in equation 21.

COLUMBIA GLACIER DATA

The principal data year for the Columbia Glacier field program was September 1, 1977, through August 31, 1978 (Mayo and others, 1979). Because the present model does not account for seasonal variations, annually averaged data are used. The middle of the data year is chosen at $t_1 = 1978.2$, at which time, the transversely averaged position of the terminus was $X = x_1 = 66.6$ km, as measured from the head of the glacier. The surface topography also was averaged transversely to form the initial longitudinal surface profile, $f_1(x)$, up to $x_k = 52.6$ km, where $\tan \alpha_{1k} = 0.039$. Above this point, the glacier consists of a broad basin receiving the flow of three large tributary branches, as shown in figures 1 and 2.

The x,y bed topography calculated by W. G. Sikonia and others (written commun., 1981) is used to obtain the valley centerline altitudes, U_j and, by using the measured glacier widths, W_{ij}, to determine the initial cross-section areas, S_{ij}.

The retreated position of the terminus is taken to be $x_m = 57.1$ km, with $\Delta x = 0.1$ km; thus, $m = 96$ and $k = 141$. Without specifying the time, t_m, the calculation of which is one of the chief results of the modeling, a final longitudinal surface profile, $f_m(x)$, is postulated. These basic variables are shown in figure 4. The graphs also show the sea-level width, $W(0)$; and area, $S(0)$; the average water depth, $\bar{h}_j$; and the width, W_{jj}, and area, S_{jj}, at x_j when $X = x_j$.

In the section entitled "Longitudinal Profiles," values are reported with up to four significant figures; these values are used because the model requires internally consistent data and because they enable the reader to check results. This is not to imply that the data are this accurate; the fluxes Q_{1k} and Q_{11} for instance, are known only to an accuracy of about 7 to 10 percent (M. F. Meier and others, written commun., 1981).

The initial flux, Q_{1k} at x_k, is estimated to be 1.354 km³/a by transversely integrating the product of glacier thickness and the downglacier component of the surface velocity. In equation 12, the value $\gamma = 0.85$ is used, as determined by Sikonia and others, (written commun., 1981). According to equation 15, the Q_{1k} is partitioned into two components, $(Q_b)_{1k} = 0.873$ km³/a and $(Q_b)_{1k} = 0.481$ km³/a, by integrating the x,y ice balance to get $(Q_b)_{1k}$ and subtracting $(Q_b)_{1k}$ from Q_{1k} to obtain $(Q_b)_{1k}$.

The measured ice balance over the lower reach is well approximated by a linear $\dot{b}(z)$ with a value of -10.68 m/a at sea level and -1.42 m/a at $z = 600$ m. When integrated over the initial surface, $f_1(x)$, in equation 10, it yields a flux component at the terminus of $(\Delta Q_b)_1 = -0.475$ km³/a for the balance over the lower reach of the glacier. The total balance flux at the terminus, thus, is 0.398 km³/a at time t_1. The transverse integration of thickness and velocity at the terminus, where γ is taken to be unity to represent pure sliding motion, gives an initial flux at the terminus of $Q_{11} = 1.343$ km³/a. Therefore, the total thinning flux at the terminus is 0.945 km³/a, and the thinning flux component for the lower reach is $(\Delta Q_h)_1 = 0.464$ km³/a.

Photogrammetric analysis of the lower reach of the glacier (Sikonia and Post, 1980) reveals the pronounced seasonal variation of calving. Figure 5 represents the transversely averaged terminus position on 26 dates from 1976.6 through 1981.7 (M. F. Meier and others, written commun., 1981). The terminus position exhibits a roughly sinusoidal seasonal variation of about 300-m amplitude, superimposed on a 1977–81 average retreat rate of about $\dot{X} = -45$ m/a.

LONGITUDINAL PROFILES

Because the present model does not independently calculate glacier flow, longitudinal surface profiles, $f_1(x)$, $f_2(x)$, . . . , $f_m(x)$, must be supplied. When the terminus is at x_i, the longitudinal profile is $f_i(x)$. Through the calving relation (equation 22), the model then determines the times, t_i, that the glacier assumes each of these m profiles.

The first two profiles are obtained from the field data, $f_1(x)$, directly, and $f_2(x)$, by transversely averaging the observed thickness change rate and then scaling the averaged thickness change rate by the initial terminus retreat rate, $\dot{X}_1 = -45$ m/a,

$$f_2(x) = f_1(x) - \frac{\dot{h}(x)\Delta x}{\dot{X}_1}, \qquad (24)$$

so that, through equations 7 to 9, $f_1(x)$ and $f_2(x)$ produce the observed $(\Delta Q_h)_1$ value. The effect of this extrapolation when $\Delta x > 45$ m is examined by varying Δx from 50 m to 500 m.

A final longitudinal profile, $f_m(x)$, is postulated by setting the flow law exponent, $n = 3$, and arbitrarily assuming that $Q_{mk} = 2Q_{1k}$. The effect of these arbitrary values is examined in the section entitled "Influence of Error in Data or Model." At $x_k = 52.6$ km, $f_m(x)$ has altitude $Z_{mk} = 430$ m, compared with the initial altitude, $Z_{1k} = 452$ m, and, at $x_m = 57.1$ km, it has cliff top altitude $Z_{mm} = 100$ m, compared with the initial cliff top altitude, $Z_{11} = 86$ m. When Columbia Glacier has retreated to $x_m = 57.1$ km, its surface area will be about 95 percent of its present value.

This $f_m(x)$ profile (figs. 4 and 6) is speculative but is glaciologically reasonable because it displays a high ice cliff and slope steepening near the terminus that is characteristic of rapidly retreating calving glaciers. Furthermore, the profile obeys equations 11 to 13 with $n = 3$ and has nearly constant flux from x_k to x_m. This $f_m(x)$ profile has a fairly high slope and produces an increased discharge with a modest thickness change, as compared with the present profile. During the period 1957–78, $\dot{h}$ at x_k was less negative compared with values farther downglacier, and, above x_k, $\dot{h}$ changed progressively to almost zero at $x = 36$ km, 16 km above x_k (Sikonia and Post, 1980). Also, Q at x_k increased during the period 1977–80 (Meier and others, written commun.); this increase is consistent with the concurrent increase in slope.

Obviously, the postulated $f_m(x)$ would not occur upon extrapolation of $f_1(x)$ and $f_2(x)$. The combination of pronounced thinning and slow retreat is believed to be a symptom of the final phase of the connection of the terminus to the shoal. This connection results in a lessening of surface slope over much of the lower reach, where the surface velocity has been observed to be slightly increasing. After a small amount of additional retreat behind the shoal, the change in the longitudinal profile is expected to undergo a transition; the profile changes will cease to produce vigorous thinning and will begin to approach $f_m(x)$. Experience with a dynamic model used

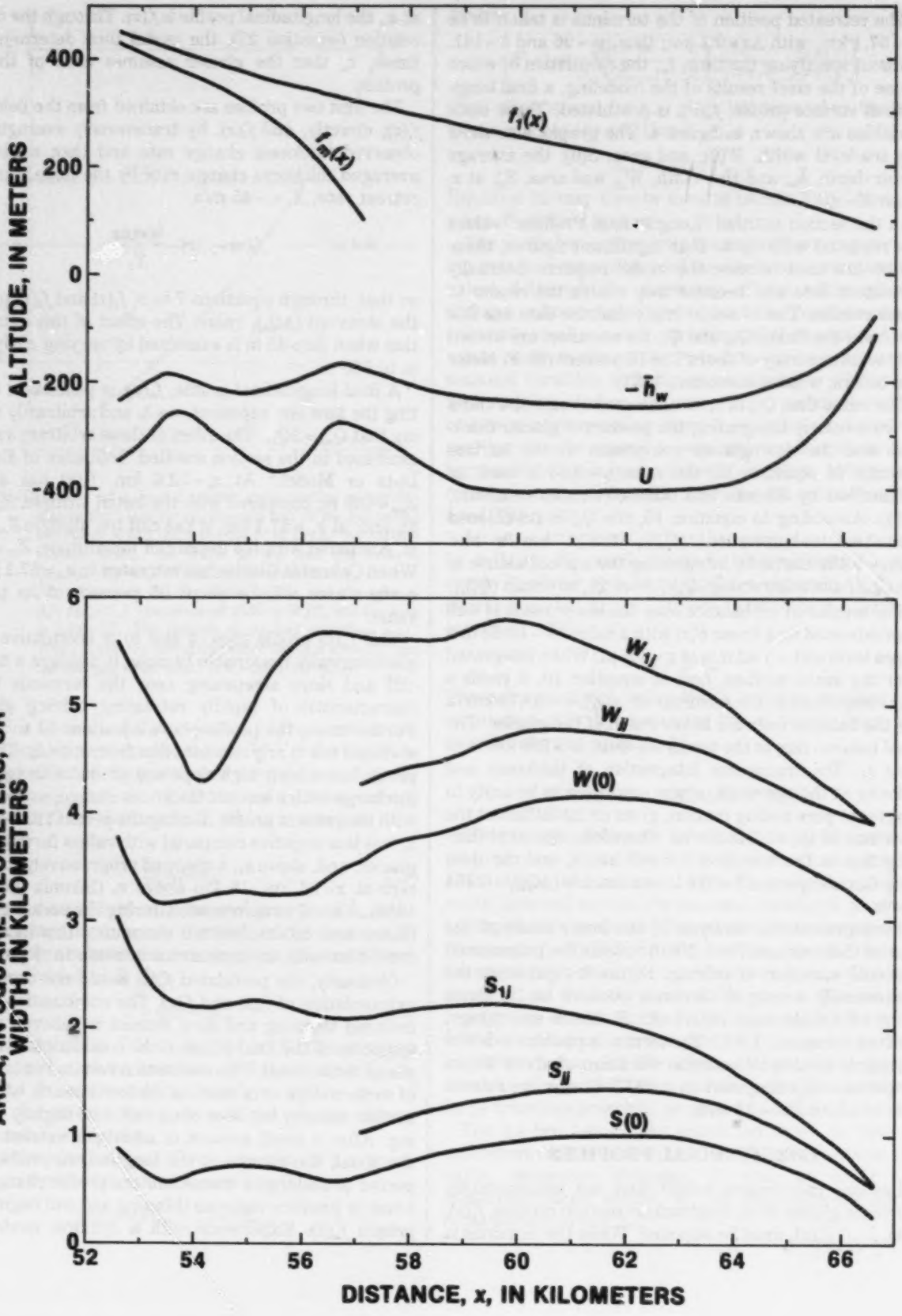
400
200
0
-200
-400
ALTITUDE, IN METERS
$f_1(x)$
$f_m(x)$
$-\bar{h}_w$
U
6
5
4
3
2
1
0
AREA, IN SQUARE KILOMETERS, OR WIDTH, IN KILOMETERS
W_{1j}
W_{jj}
W(0)
S_{1j}
S_{jj}
S(0)
52
54
56
58
60
62
64
66
DISTANCE, x, IN KILOMETERS

with Columbia Glacier data also suggests the existence of this transition (R. A. Bindschadler, written commun., 1981). Figure 6 gives the set of longitudinal profiles interpolated between $f_1(x)$ and $f_m(x)$; shown are the $f_i(x)$ profile for $i=1, 2, 3, 4, 5, 6, 11, 16, 21, 26, \ldots, 91, 96=m$. The interpolation was made so that the $f_i(x)$ profiles changed smoothly from $f_1(x)$ to $f_m(x)$, embodied the transition, and were free of waves; that is, at any x, the surface altitude was always decreasing with time.

The influence on the solution of the arbitrariness of this interpolation is examined by considering alternative interpolations; alternative $f_m(x)$ profiles also are considered. In fact, considerable uncertainty is involved in all the values used to describe the Columbia Glacier; the effect of such errors is the subject of the section "Influence of Error in Data or Model" of this report.

CALCULATED TERMINUS RETREAT

The section entitled "Longitudinal Profiles" describes the data adopted as the prime case (case 1). Setting $X_1=-45$ m/a not only leads, through the effect of equation 24 on $f_2(x)$, to the formation of a set of longitudinal profiles, $f_i(x)$, but also provides a condition for determining the value of the calving coefficient, c. If $X=-45$ m/a is taken to apply not only at t_1, but also until $X=x_2$, then

$$t_2=t_1-\Delta x/\dot{X}_1=1978.2+100/45=1980.4 \qquad (25)$$

is the required condition, which is met when $c=28.3$ per year. This value is close to the average value of 27 ± 2 per year derived from observations of many Alaska glaciers (C. S. Brown and others, written commun., 1981).

The sensitivity of the model to the value of c is shown in figure 7, which displays $X(t)$ for three different values of c used with the case 1 data and displays the corresponding three $Q_c(t)$ curves.

The results of the calculations for $c=28.3$ a^{-1} using the case 1 data are further illustrated in figures 8 and 9. Shown in figure 8 are the flux components at the terminus from above $x_4=52.6$ km and from the lower reach, as well as the retreat rate and calving and average glacier speeds. A maximum retreat rate of about $\dot{X}=-4.1$ km/a occurs in early 1983, and the total volume, R, removed from the reservoir of ice above x_4 is 6.0 km^3. A maximum calving flux of $Q_c=9.9$ km^3/a occurs at $t=1983.5$. Figure 9 shows the longitudinal profiles, $f_i(x)$, assumed by the glacier at selected times during the retreat from $x_1=66.6$ km to $x_m=57.1$ km.

FIGURE 4.—Longitudinal geometry of lower reach of Columbia Glacier, Alaska. At time $t_1=1978.2$, when the terminus is at $x_1=66.6$ km, the surface profile is $f_1(x)$, the width is W_{t_1}, and the cross-section area is S_{t_1}. At time, t_m, when the terminus is at $x_m=57.1$ km, the surface profile is $f_m(x)$. At sea level, the width is $W(0)$, and the area is $S(0)$. The centerline bed altitude is U, and the average water depth is $h_w=S(0)/W(0)$. The W_{t_i} curve and S_{t_i} curve give, at each x_i, the width and cross-section area when the terminus is at x_i.

INFLUENCE OF ERROR IN DATA OR MODEL

EFFECT OF INDIVIDUAL ERRORS

To investigate the effect of possible errors in the data or assumptions used in the model on the calculated $X(t)$ and $Q_c(t)$ results, several cases were created by varying one or another of the components of the data. Each case, except for the adjustment stated for it, consists of the same data used for case 1. The size of each data adjustment is approximately equal to the expected observational error (W. C. Sikonia and others, written commun., 1981).

Case 2 includes four subcases for different variations of the volume balance function, $b'(z)$. Case 2a uses a 1-m/a more positive $b'(z)$, along with an initial flux, Q_{1a}, decreased by 0.072 km^3/a to preserve the initial flux, Q_{11}, at the terminus. Case 2b is the opposite, with $b'(z)$, made more negative by 1 m/a and Q_{1a} increased by 0.072 km^3/a. Case 2c uses a steeper $b'(z)$, with -11.41 m/a at sea level and -0.51 m/a at $z=600$ m, which preserves the initial flux component, $(\Delta Q_b)_1=-0.475$ km^3/a, contributed by the balance over the lower reach. Case 2d uses a shallower $b'(z)$, with -9.95 m/a at sea level and -2.32 m/a at $z=600$ m, which also preserves $(\Delta Q_b)_1$. Figure 10 shows the original $b'(z)$ function along with those for cases 2a, 2b, 2c, and 2d. Steeper is defined as a rapid increase in balance with increasing z; by shallower, a slower increase.

Case 3a uses a Q_a increased by 8 percent, and case 3b uses a Q_a decreased by 8 percent. The variation is applied to the initial value $Q_{1a}=1.354$ km^3/a and, through equation 13, proportionately scales all the Q_a values. The variation also additively modifies all the Q_U by $\pm0.08\ Q_{1a}$.

Case 4a uses a shallower bed topography, with U_f increased by 40 m for $x\leq65.6$ km. Case 4b uses a deeper bed topography, with U_f decreased by 40 m for $x\leq65.6$ km. Each of these variations is accompanied by a linear function of x ($x>65.6$ km) that reduces the variation to zero at $x_1=66.6$ km. These two cases are shown as figure 11.

Case 5a uses a shallower shoal, raised by adding a linear function of x that decreases from 10 m at $x_1=66.6$ km to zero at $x=65.6$ km. Case 5b uses a deeper shoal, lowered by the opposite application of the same linear function. These two cases are shown as figure 12.

Cases 2 to 5 all use the same set of longitudinal profiles, $f_i(x)$, as case 1.

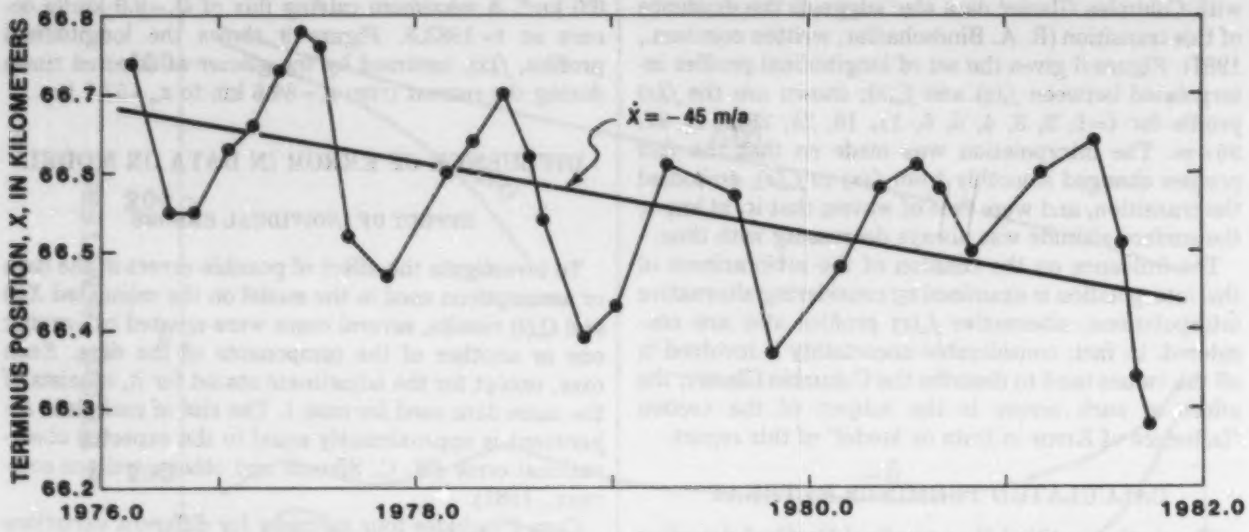

FIGURE 5.—Position of the terminus as a function of time. Position $X(t)$ is averaged over a 3.5-km width of active ice. The heavy line corresponds to $\dot{X} = -45$ m/a. The measurement error in X at each data point is approximately equal to the diameter of the dot (15 m).

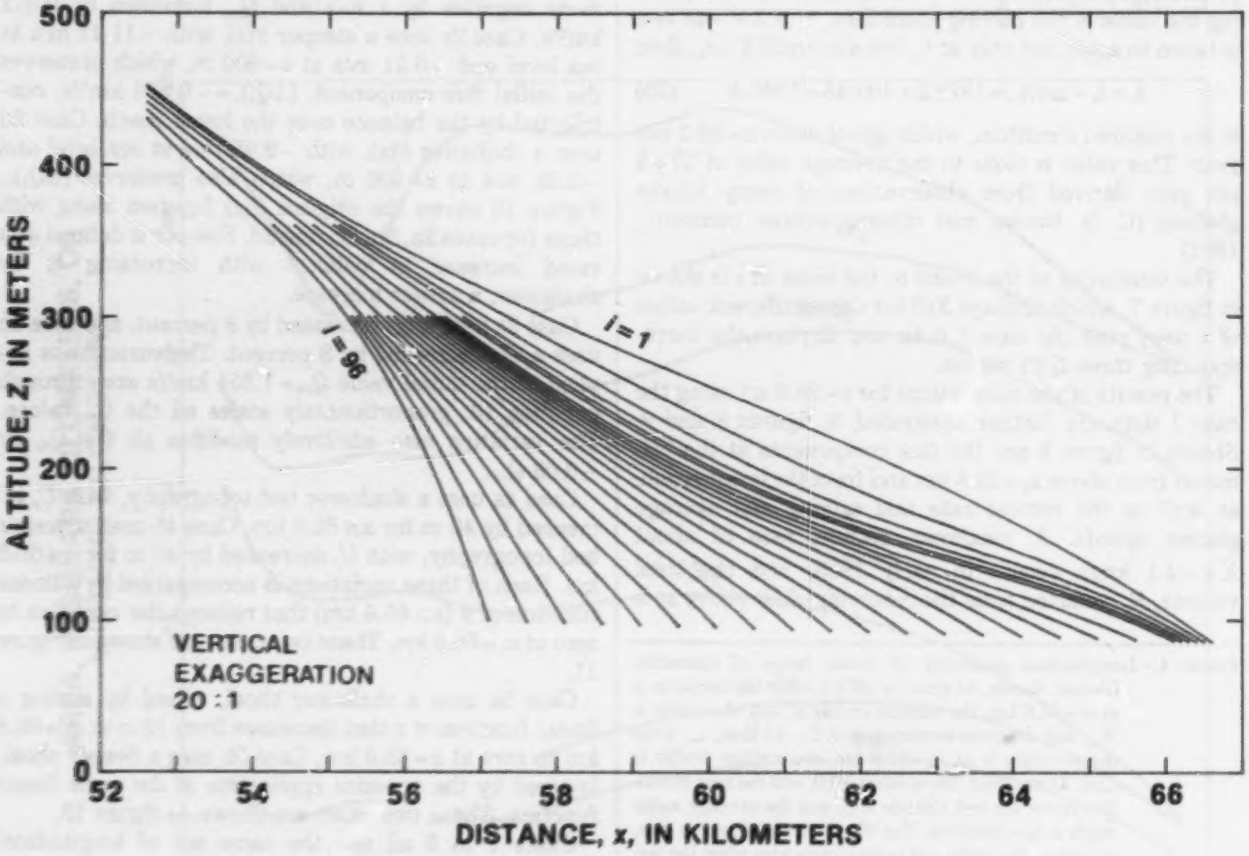

FIGURE 6.—Prime set (case 1) of postulated longitudinal profiles $f(x)$ for $i = 1, 2, 3, 4, 5, 6, 11, 16, \ldots, 91, 96$.

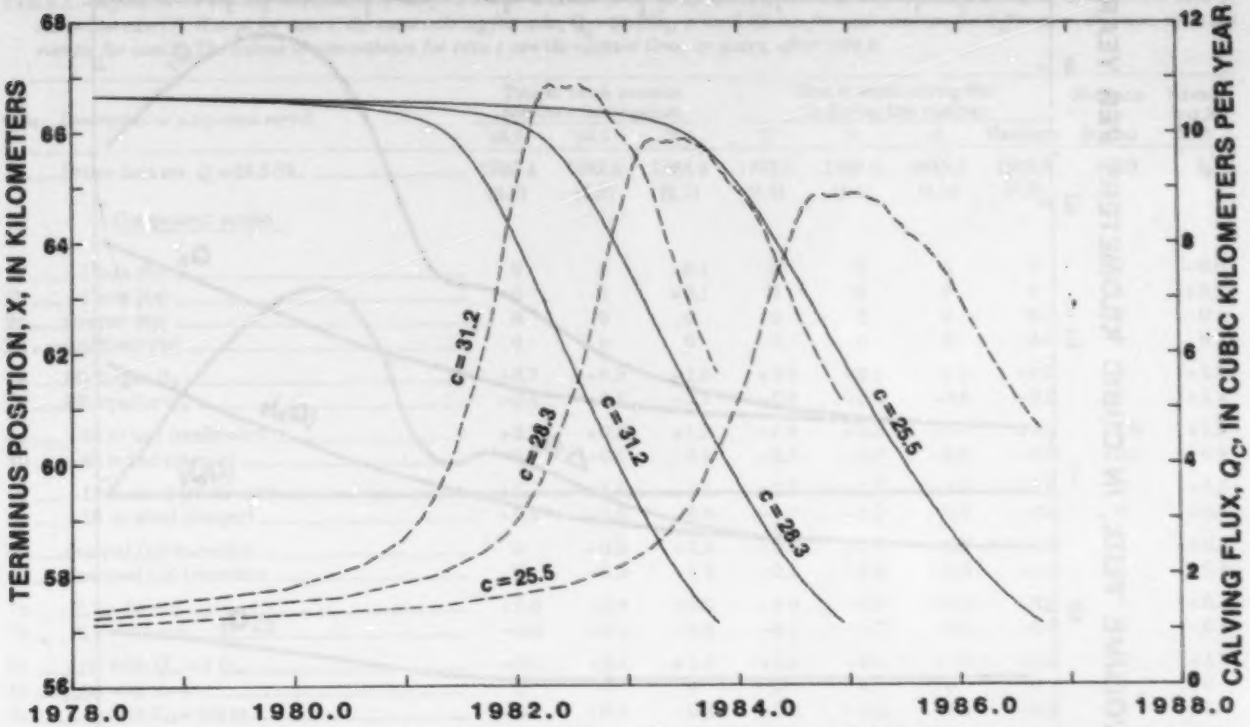

FIGURE 7.—Sensitivity of the model results to the value of the calving coefficient c using the case 1 data. The terminus retreat, $X(t)$, and the calving flux, $Q_c(t)$, are shown for $c = 25.5$, 28.3, and 31.2.

Case 6a uses a set of longitudinal profiles, $f_i(x)$, that delays the transition from continuing vigorous thinning to beginning to approach $f_m(x)$. Case 6b uses a set that hastens the transition. These two sets of longitudinal profiles are shown as figures 13 and 14, which show the $f_i(x)$ for the same i values as in figure 6.

Case 7a uses a 20 percent smaller initial retreat rate, $\dot{X}_1 = -36$ m/a, which produces $t_2 = 1981.0$. Case 7b uses a 20 percent larger initial retreat rate, $\dot{X}_1 = -54$ m/a, which produces $t_2 = 1980.0$. These varied initial retreat rates, through the effect of equation 24 on $f_2(x)$, require the formation of modified sets of longitudinal profiles. The profiles for cases 7a and 7b are shown in figures 15 and 16, respectively; the $f_i(x)$ shown are for the same i values as in figure 6.

Case 8 includes three subcases for variation of the longitudinal profile, $f_m(x)$, for the retreated terminus position. They were constructed, as were the $f_m(x)$ used for case 1, by using equations 11 and 12 and the assumed bed topography to produce nearly constant flux between $x_s = 52.6$ km and $x_m = 57.1$ km. Case 8a uses an $f_m(x)$ that assumes $Q_{ms} = 3Q_{1s}$ instead of $2Q_{1s}$. Case 8b uses an $f_m(x)$ that assumes the flow law exponent $n = 4$ instead of 3. Case 8c uses an $f_m(x)$ that assumes $Z_{ms} = 420$ m rather than 430 m. These cases are shown, along with the basic $f_m(x)$, as figure 17. They each lead to a different set of longitudinal profiles, $f_i(x)$, that, except for $i = m$, closely resembles the set for case 1.

The results for these cases are summarized in table 1, which gives several significant points on the $X(t)$ and $Q_c(t)$ curves for case 1 and also gives the differences from those values for cases 2 to 8. Because, from equation 19, the calving flux depends only on the calving coefficient, c, and on the cross-section geometry, $S\bar{h}_x$, the dependence of Q_c on x will be the same for all cases in which only data components other than c and $S\bar{h}_x$ are varied. Such variations may change $X(t)$ and, therefore, $Q_c(t)$, but $Q_c(x)$ is unchanged. Also included is R, the total volume of ice removed from above $x_s = 52.6$ km, as given by equation 16 and 17.

As is shown in table 1, several of the variation cases significantly affect t_2 when the same value of the calving coefficient is used as in case 1. Because the condition $t_2 = 1980.4$ is considered to be more reliable than the value $c = 28.3$, the coefficient should be adjusted in the variation cases so that the condition is still met. Table 2 shows the revised results for those cases that, for $c = 28.3$, give a t_2 significantly different from 1980.4; they are denoted by a prime.

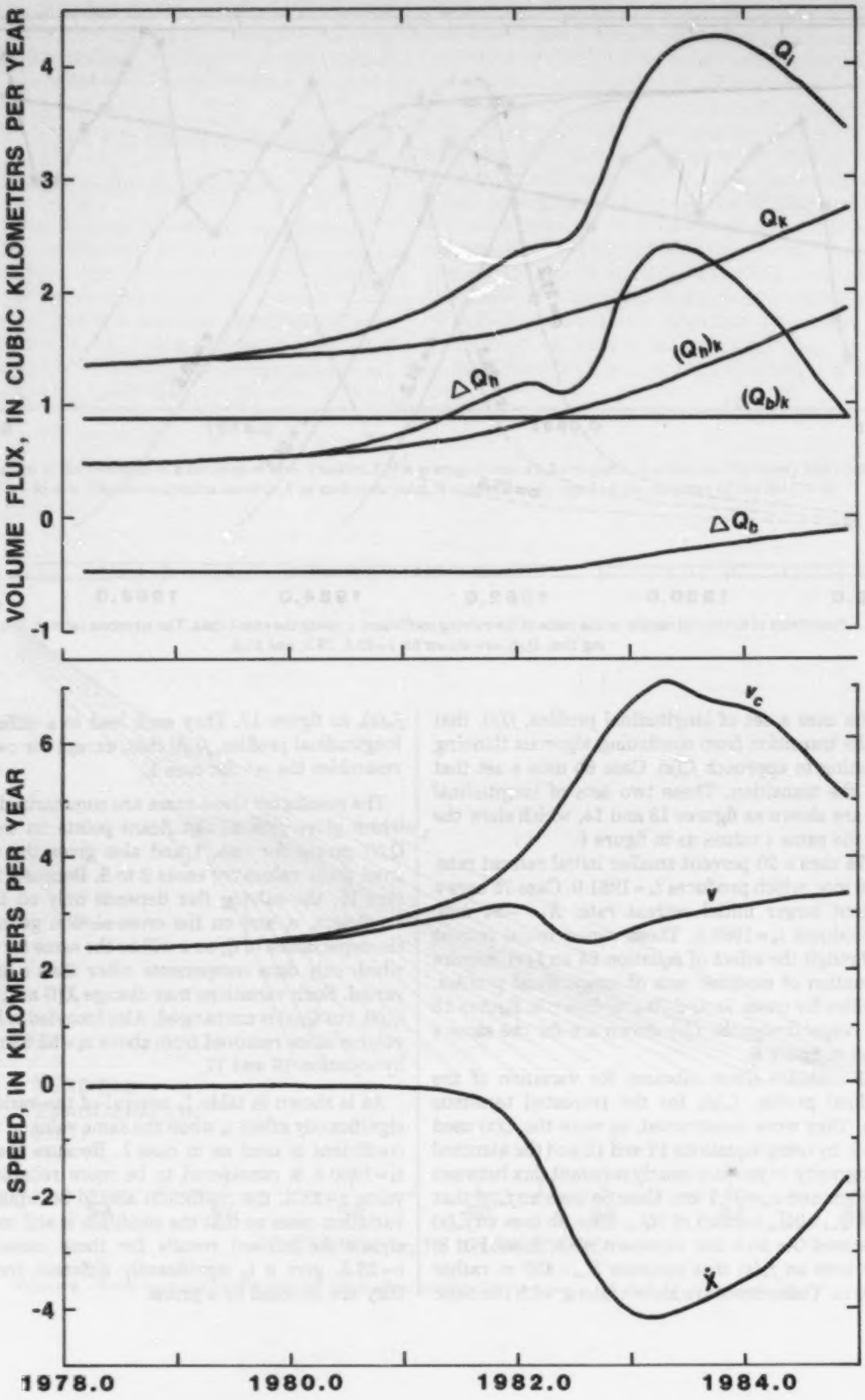
VOLUME FLUX, IN CUBIC KILOMETERS PER YEAR
4
3
2
1
0
-1
Q_t
Q_k
$(Q_h)_k$
$(Q_b)_k$
ΔQ_h
ΔQ_b
SPEED, IN KILOMETERS PER YEAR
6
4
2
0
-2
-4
v_c
v
$\dot{x}$
1978.0
1980.0
1982.0
1984.0

TABLE 1.—*Effect on the calving calculation of varying one or another of the components of the data while holding all others at the values used in the prime case (1). Except for case 9, the same calving formula, $Q_c = 28.3Sh_w$, is used. Shown for each case are the differences, in years, from the results for case 1. The values in parentheses for case 1 are the elapsed time, in years, after 1978.2*

Case	Description or component varied	Time at which terminus position x (km) reaches: 66.5	65.6	57.1	Time at which calving flux Q_c (km³/a) first reaches: 3	6	9	Maximum	Maximum Q_c (km³/a)	Volume loss R km³)
1	Prime data set, $Q_c = 28.3\,Sh_w$	1980.4 (2.2)	1982.4 (4.2)	1984.9 (6.7)	1982.0 (3.8)	1982.6 (4.4)	1983.0 (4.8)	1983.5 (5.3)	9.9	6.0
	Component varied									
2a	+1 m/a $\dot{b}(x)$	0	0	−0.1	0	0	0	0	0	−0.8
2b	−1 m/a $\dot{b}(x)$	0	0	+0.1	0	0	0	0	0	+0.7
2c	steeper $\dot{b}(x)$	0	0	0	0	0	0	0	0	0
2d	shallower $\dot{b}(x)$	0	0	0	0	0	0	0	0	0
3a	8% larger Q_a	+0.7	+0.9	+1.0	+0.9	+0.9	+0.9	+0.9	0	+1.7
3b	8% smaller Q_a	−0.4	−0.6	−0.7	−0.6	−0.6	−0.6	−0.6	0	−1.4
4a	+40 m bed (shallower)	+0.2	+0.6	+1.9	+0.8	+0.9	——	+0.9	−1.8	+1.5
4b	−40 m bed (deeper)	−0.2	−0.5	−0.9	−0.5	−0.7	−0.8	−0.6	+2.0	−0.9
5a	+10 m shoal (shallower)	+1.1	+1.5	+1.5	+1.5	+1.5	+1.5	+1.5	0	+0.8
5b	−10 m shoal (deeper)	−0.6	−0.8	−0.8	−0.9	−0.8	−0.8	−0.8	0	−0.5
6a	delayed $f_s(x)$ transition	0	+0.3	+0.3	+0.2	+0.3	+0.3	+0.3	0	+0.2
6b	hastened $f_s(x)$ transition	0	−0.3	−0.3	−0.3	−0.3	−0.3	−0.3	0	−0.1
7a	$\dot{X}_1 = -36$ m/a	+0.6	+0.9	+0.8	+0.9	+0.9	+0.8	+0.8	0	+0.5
7b	$\dot{X}_1 = -54$ m/a	−0.4	−0.7	−0.8	−0.7	−0.7	−0.6	−0.6	0	−0.3
8a	$f_m(x)$ with $Q_{m_0} = 3\,Q_{t_0}$	+0.2	+0.5	+1.0	+0.4	+0.5	+0.5	+0.6	0	+4.3
8b	$f_m(x)$ with $n = 4$	0	0	0	0	0	0	0	0	0
8c	$f_m(x)$ with $Z_{m_0} = 420$ m	−0.1	−0.2	−0.2	−0.2	−0.2	−0.2	−0.2	0	−0.5
9	Prime, but $Q_c = 19.7\,Sh_w$	0	−0.2	−0.6	−0.2	−0.4	−0.5	−0.4	+1.6	−0.8

Case 2 has negligible effect except that cases 2a′ and 2b′, through their adjustments of Q_{m_0}, make a change in R of about ±12 percent.

Case 3, if c is not adjusted to maintain $t_1 = 1980.4$, results in a large initial change to $X(t)$ when X is weak and, thereafter, a slight progressive growth of that change. In case 3a, for example, when the Q_{m_0} are increased by 8 percent, more flux is produced at the terminus; through equation 18, this makes $\dot{X}$ less negative and slows retreat. If, for either case 3a′ or case 3b′, c is adjusted to make $t_2 = 1980.4$, then, for $t > t_2$, the variation made to the Q_{m_0} is slightly over balanced, as shown in tables 1 and 2.

Case 4, if c is not adjusted to maintain $t_2 = 1980.4$, results in a progressive change to $X(t)$. In case 4a, for example, when the bed $U(x)$ is made shallower (see fig. 11), the Q_c term is reduced through equation 19, which makes $\dot{X}$ less negative and slows retreat. If, for either case 4a′ or case 4b′, c is adjusted to make $t_2 = 1980.4$, then, for $t > t_2$, the effect is diminished to about half. The adjustment to c that compensates for the smaller change in $U(x)$ for $x_2 \le x \le x_1$ is overmatched by the larger change to $U(x)$ for $x < x_2$. The $X(t)$ and $Q_c(t)$ curves for these cases and the curves for case 1 are shown in figure 18.

Case 5, if c is not adjusted to maintain $t_2 = 1980.4$, results in a large change to $X(t)$ over $x_2 \le x \le x_1$, where the variation of $U(x)$ occurs and, thereafter, a slight progressive growth of that change. In case 5a, for example, when the shoal is raised (see fig. 12), the Q_c term is reduced through equation 19, which makes $\dot{X}$ less negative and slows retreat. If, for either case 5a′ or case 5b′, c is adjusted to make $t_2 = 1980.4$, then, for $x < x_2$, the adjustment operates on the original $U(x)$ and produces a result of the opposite sign. That is, if c is increased to compensate for a shallower shoal and make the terminus reach x_2 at $t_2 = 1980.4$, then the larger c causes the terminus to traverse the remaining distance, where $U(x)$ has not been varied, at a greater rate than in case 1. The $X(t)$ and $Q_c(t)$ curves for these cases and the curves for case 1 are shown in figure 19.

FIGURE 8.—Features of the calculations for $c = 28.3$, using the case 1 data. Shown are the balance flux, $(Q_a)_x$, and thinning flux, $(Q_s)_x$, components of the total flux, Q_x, into the lower reach from above $x_x = 52.6$ km; the flux components due to the balance, ΔQ_a, and the thinning flux, ΔQ_s, over the lower reach; and the total flux at the terminus, Q_t. Also shown are the average glacier speed at the terminus, v; the calving speed, v_c; and their difference (the retreat rate), $\dot{X}$.

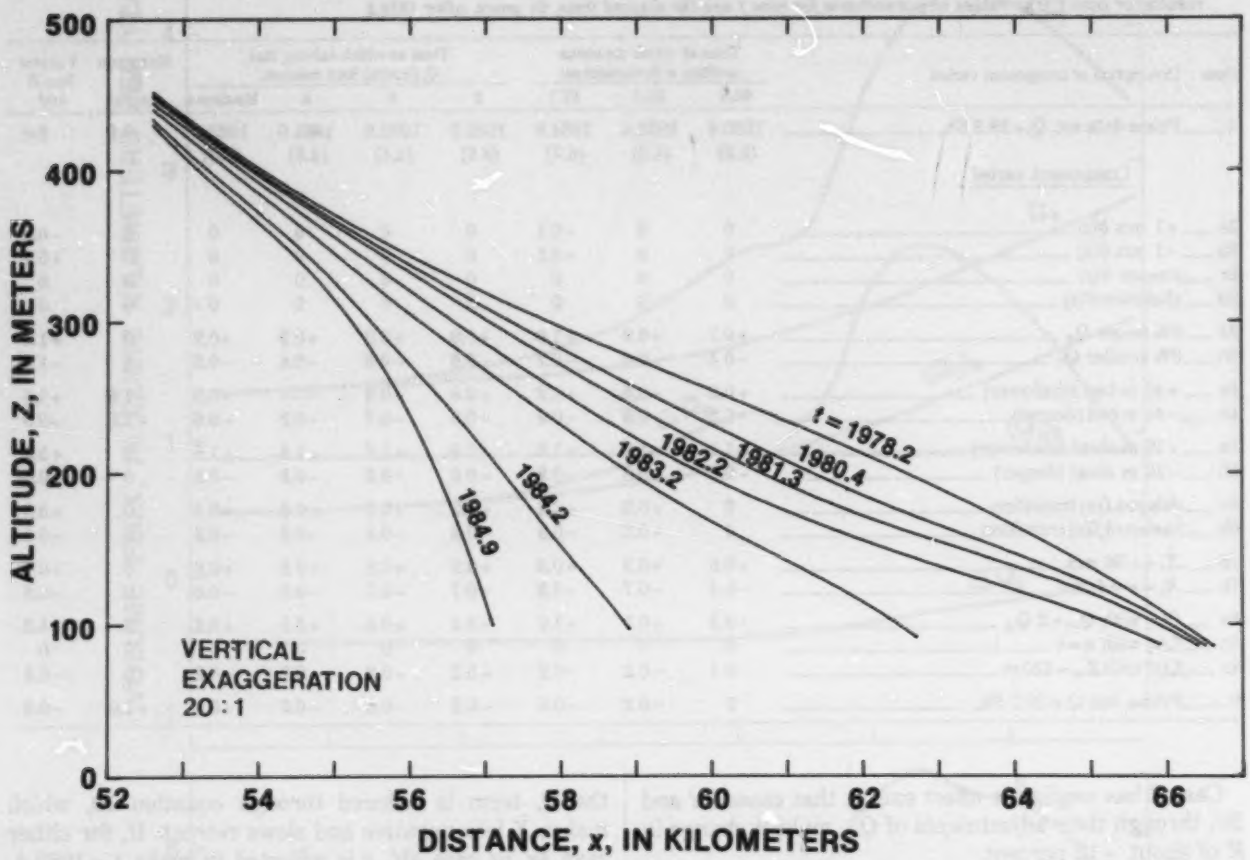

FIGURE 9.—Longitudinal profiles assumed by the glacier in the calculations using the case 1 data and $c = 28.3$. The $f(x)$ are shown for $t = 1978.2$, 1980.4, 1981.3, 1982.2, 1983.2, 1984.2, and 1984.9.

TABLE 2.—*Effect on the calving calculation of varying one component of the data and simultaneously adjusting* c, *as indicated, to constrain the solution to pass through* $x = 66.5$ *km at* $t_2 = 1980.4$. *Shown for each case are the differences, in years, from the result for case 1*

Case	c	Time at which terminus position x (km) reaches:			Time at which calving flux Q, (km³/a) first reaches:				Maximum Q, (km³/a)	Volume loss R (km³)
		66.5	65.6	57.1	3	6	9	Maximum		
3a′	30.6	0	−0.1	−0.3	−0.1	−0.2	−0.2	−0.2	+0.8	+0.6
3b′	26.1	0	+0.1	+0.3	+0.1	+0.2	+0.3	+0.2	−0.8	−0.7
4a′	29.0	0	+0.3	+0.9	+0.4	+0.5	——	+0.5	−1.6	+1.1
4b′	27.6	0	−0.2	−0.6	−0.3	−0.4	−0.5	−0.4	+1.7	−0.7
5a′	32.1	0	−0.2	−0.6	−0.2	−0.3	−0.4	−0.3	+1.3	−0.7
5b′	25.2	0	+0.2	+0.7	+0.2	+0.3	——	+0.4	−1.1	+0.8
6a′	29.0	0	+0.2	+0.6	+0.1	+0.2	+0.2	+0.2	+0.2	+3.8
6b′	28.0	0	−0.1	−0.1	−0.1	−0.1	−0.1	−0.1	−0.1	−0.4

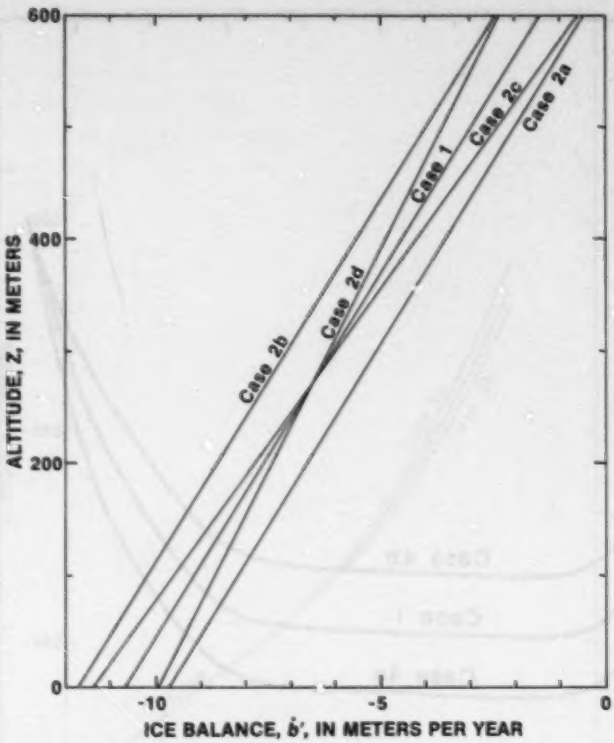

FIGURE 10.—Volume balance functions, $\dot{b}'(x)$, for case 1, 2a, 2b, 2c, and 2d.

Case 6 does not affect t_2 because the first two longitudinal profiles, $f_1(x)$ and $f_2(x)$, are the same as those in the $f_i(x)$ used with case 1. The main effect of the variation of the $f_i(x)$, as shown in figures 13 and 14, is on the relation of volume change to terminus position, dV/dX. Through equation 9, this controls the flux component, ΔQ_a, at the terminus contributed by the thinning of the lower reach, but the total volume lost to thinning is unchanged by this variation. Therefore, the retreat rate is decreased and then increased (case 6a), or it is increased and then decreased (case 6b); in either case, only a small change to $X(t)$ results.

Case 7 varies the initial retreat rate, $\dot{X}_1$, and, thus, by definition, presumes a proportionately different t_2. As in case 6, the variation produces a retreat rate that slightly decreases and then slightly increases (case 7a) or that slightly increases and then slightly decreases (case 7b). The resulting $X(t)$ and $Q_x(t)$ curves and the curves for case 1 are shown in figure 20.

Case 8 demonstrates that little effect is caused by the variations to $f_i(x)$ for $i \approx m$. Case 8a, though, does show a pronounced slowing of the retreat rate. Unlike case 3a, which assumes a Q_a that ranges from 1.08 to 2.16 times the Q_{1a} used with case 1, case 8a assumes a range from 1.00 to 3.00 times that Q_{1a} value. Although case 8a attains a much higher Q_a than does case 3a, the increase occurs when i is large (when the retreat rate is great) and, thus, has only a small effect on $\dot{X}$ and $X(t)$; this is the condition $F \gg 0$ in equations 21 and 22. Because case 8a has Q_a only slightly larger than in case 1 when i is small, it produces a progressively slowing retreat rate when compared with case 1. When c is adjusted to maintain $t_2 = 1980.4$, the effect is reduced to about half. The $X(t)$ and $Q_x(t)$ curves for the c-adjusted case 8a', for case 1, and for the c-adjusted case 8c' are shown in figure 21.

Case 9 uses the alternative form of the calving relation given by equation 23. If the coefficient is chosen to have $t_2 = 1980.4$ when the glacier data for case 1 are used, then $\hat{c} = 19.7$; the $X(t)$ curve produced is not identical to that of case 1 because $\bar{h}_w/h_w$ is not constant with x. That ratio varies according to the variation with x of the valley cross-section shape, as given by equations 4 to 6.

The volume loss, R, above $x_h = 52.6$ km differs from case to case mainly because of the time, $t_m - t_1$, required for the terminus to retreat to $x_m = 57.1$ km. A second order effect on the response of R depends on whether a particular case differs more from case 1 during the early phase of retreat, when Q_a is small, or during the late phase of retreat, when Q_a is large. This difference in response exists because Q_a is a function of longitudinal profile, $f_i(x)$, and, thus, of terminus position, X_i, rather than of time.

EFFECT OF SUPERIMPOSED ERRORS

In the first phase of the sensitivity analysis, each variation was considered separately to examine the nature of its effect singly on the $X(t)$ and $Q_x(t)$ curves. A second phase of the analysis takes into account the possibility that several of these errors may actually exist together in the data used here and that the curves should be accompanied by an estimate of the resultant summation of the effects of the individual errors. Each of the cases in this second phase of analyses is constructed on the presumption that the magnitude of the variation used is representative of the likely error in the quantity varied, as based on field program experience and glaciological judgment. The term "likely" is used in place of normal statistical measures of error, such as standard or probable, because many kinds of errors due to measurement or assumption cannot be defined quantitatively on the basis of known, or knowable, statistical distributions.

A resultant error is estimated for $X(t)$ by assuming that there exists some particular, but as yet unspecified, probability, p, to which the term "likely error" pertains. When one case at a time is considered, the response of $X(t)$ is caused entirely by the variation imposed on the

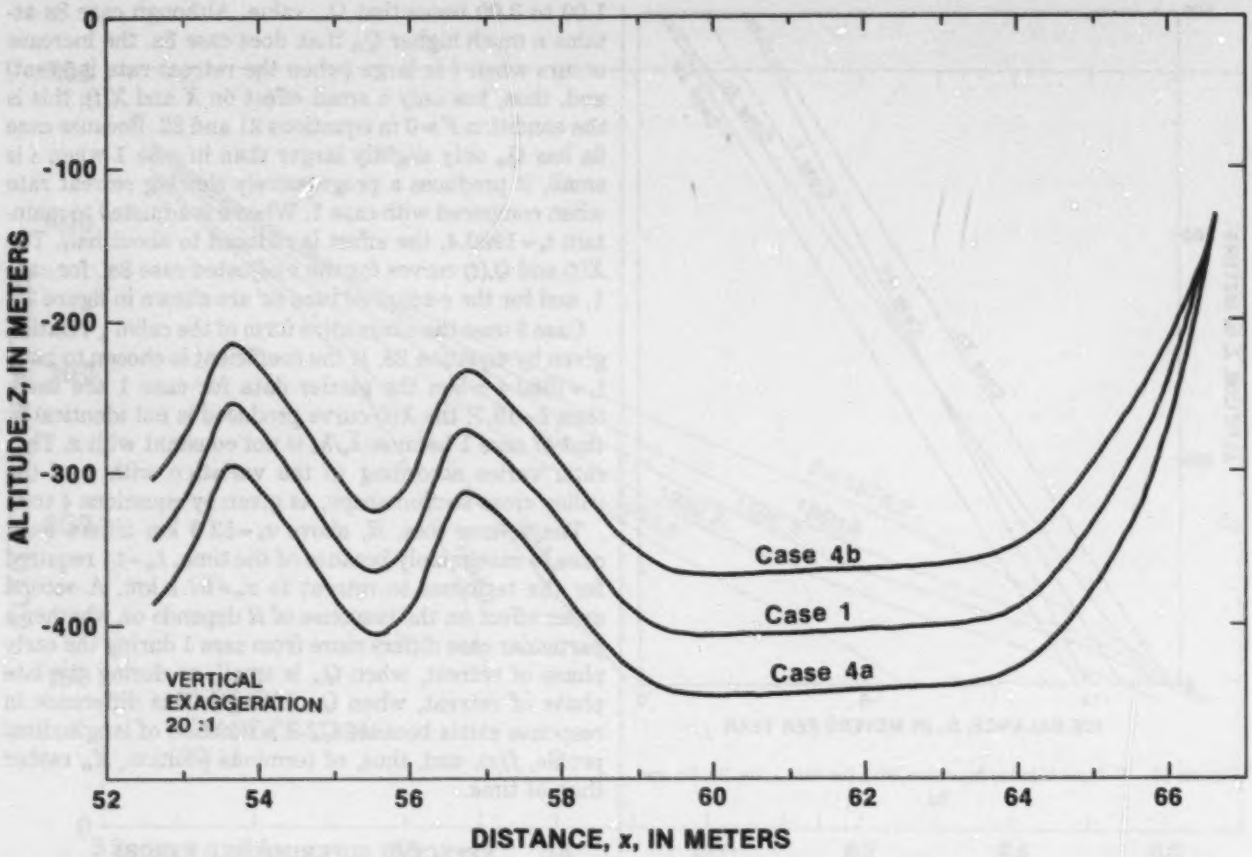

FIGURE 11.—Centerline bed altitude profiles, $U(x)$, for cases 1, 4a, and 4b.

defining data; thus, the same probability can be imputed to the resulting $X(t)$ curve as is assumed for the data variation that produced it. Because the model constitutes a mildly nonlinear, but continuous, transformation of the data (that is, as shown in tables 1 and 2, $X(t)$ does not respond exactly linearly to variations in the defining data), the two distributions are actually slightly different. If, however, a normal distribution is assumed to be reasonably valid, then p can be expressed in terms of $M(p)$ standard deviations. Provided that the other cases are c adjusted to maintain $t_3 = 1980.4$, so that they share none of the $\dot{X}_1$ variation that is the subject of case 7, the cases are assumed to be statistically independent of each other.

Considering, first, only those subcases (I) that produce faster retreat than case 1, let

$$t_{j1} - t_{jI} = MG_{jI}, \tag{26}$$

where t_{jI} denotes the time when $X = x_j$ for some subcase I and where G_{jI} is the standard deviation of the t_{jI} values about t_{j1} for that subcase. Since the variance of the sum of uncorrelated variables is the sum of the variances of those variables, the time, t_{jR}, for the resultant summation of the effect of the individual errors is given by

$$t_{j1} - t_{jR} = M\left[\sum_I G_{jI}^2\right]^{1/2} = M\left[\sum_I (t_{j1} - t_{jI})^2/M^2\right]^{1/2} = \left[\sum_I (t_{j1} - t_{jI})^2\right]^{1/2}. \tag{27}$$

Then, using the t_{jR} for $1 \le j \le m$, the curve $X_R(t)$ is constructed as an estimation of likely early retreat. Without having explicitly stated p, or the corresponding M, the curve $X_R(t)$ is at the same probability level as denoted by the term "likely error." The estimated likely late retreat curve, $X_L(t)$, is constructed similarly by summing over only those subcases that produce slower retreat than case 1. The curves $X_R(t)$ and $X_L(t)$ are shown, and the $X(t)$ for case 1, in figure 22. This approach to estimating $X_R(t)$ and $X_L(t)$ is undertaken as a simpler alternative to mak-

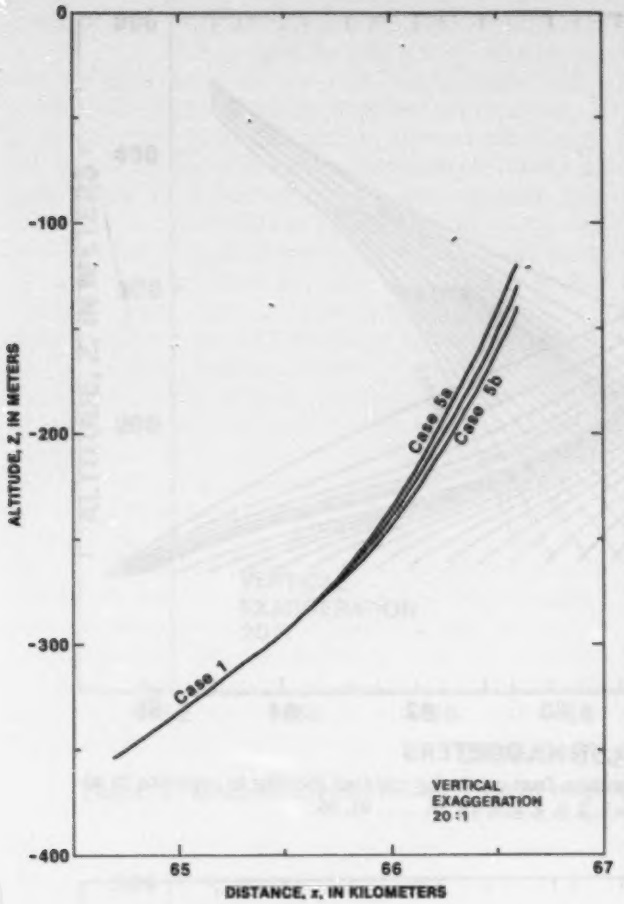

FIGURE 12.—Shoal bathymetry, $U(x)$, for cases 1, 5a, and 5b.

ing an extensive stochastic simulation with data not well enough known to justify such treatment.

EFFECT OF NUMERICAL ERROR

The numerical treatment of the data for $\Delta x = 100$ m introduces a truncation error that is smaller than the resolution at which the values are reported in tables 1 and 2. Those values are given to tenths, and the truncation error is a fraction of a tenth. The truncation error value was determined by making the calculations for case 1 with defining data specified at equally spaced x_i for $\Delta x = 500$ m, 250 m, 100 m, and 50 m. Several significant features of the solution are shown in table 3 for each of the four Δx values.

TABLE 3.—*Effect on the solution due to truncation error*

	Data spacing Δx			
	50 m	100 m	250 m	500 m
Time terminus reaches:				
$x = 65.6$ km	1982.40	1982.36	1981.90	1981.22
$x = 57.1$ km	1984.96	1984.93	1984.46	1983.79
Time calving flux first reaches:				
$Q_c = 3$ km³/a	1982.04	1982.01	1981.55	1980.85
$Q_c = 6$ km³/a	1982.65	1982.62	1982.15	1981.45
$Q_c = 9$ km³/a	1983.04	1983.00	1982.54	1981.85
Total discharge (km³) into lower reach through $x = 52.6$ km	11.90	11.87	11.26	10.36
Volume loss, R (km³), above $x = 52.6$ km	6.00	5.99	5.80	5.48

DISCUSSION

This model uses the equation of continuity to predict the retreat rate of the Columbia Glacier and largely avoids uncertainties involved in glacier dynamics such as calculating the magnitude of sliding velocity at the glacier bed or the flow law of ice deforming in a highly transient mode. However, the model avoids these uncertainties at the cost of needing to specify a somewhat arbitrary set of longitudinal profiles. The sensitivity analysis shows that the different geometrical assumptions involved in constructing these profiles have some effect on the timing of retreat but little effect on the form of the retreat curve or the calving flux curve. These effects are, in fact, less than the effects of some uncertainties in the data.

The model is based on information collected during the 1977–78 measurement year, except for the value of terminus retreat, X, which is the average over 4.5 years of record. The observed change in the glacier since 1978 generally is consistent with the change expected. For instance, the ice discharge, Q_c, at the upglacier limit of the model was observed to increase by 7.8 percent from the 1977–78 measurement year to the 1979–80 measurement year (Meier and others, written commun., 1981); the expected increase (see fig. 8) was 7.4 percent.

Calving at the terminus, however, was much less in 1980 than expected. Calving appears to be related to meltwater runoff (Sikonia and Post, 1980; Sikonia, in press). In the summer of 1980, the coldness and heavy snowfalls presumably decreased summer runoff. Furthermore, the outlet stream moved east, out of the main channel, and, as a result, the embayment was not extended upglacier. During the winter of 1980–81, the seasonal advance appeared to be ahead of expectation. However, rapid embayment formation during the summer of 1981 caused unusually rapid terminus retreat,

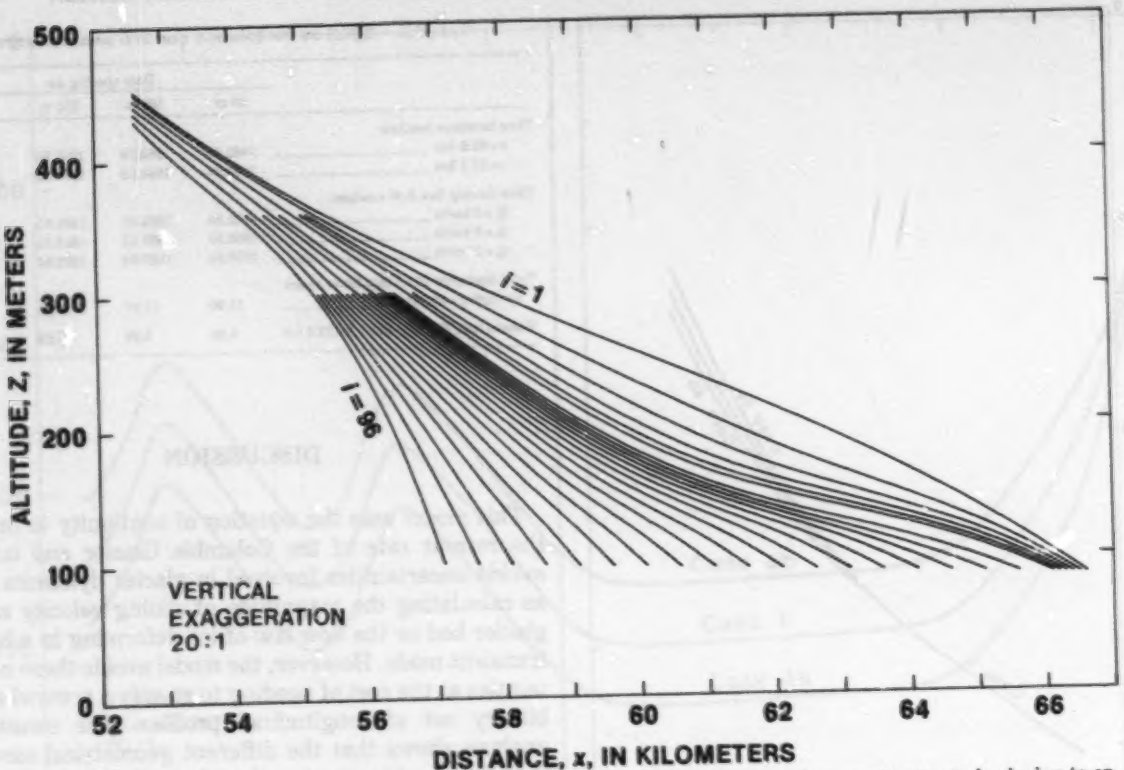

FIGURE 13.—Longitudinal profiles for case 6a that delay the transition from continuing vigorous thinning to beginning to approach $f_\infty(x)$. The $f_i(x)$ are shown for $i = 1, 2, 3, 4, 5, 6, 11, 16, \ldots, 91, 96$.

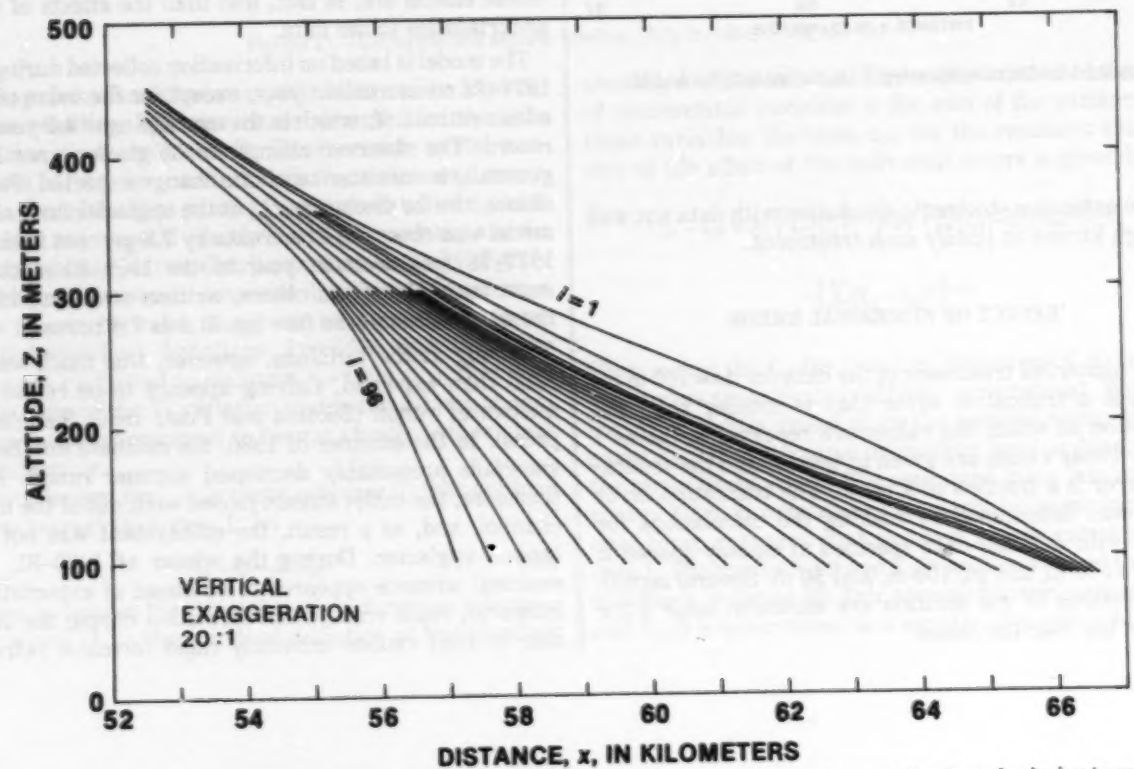

FIGURE 14.—Longitudinal profiles for case 6b that hasten the transition from continuing vigorous thinning to beginning to approach $f_\infty(x)$. The $f_i(x)$ are shown for $i = 1, 2, 3, 4, 5, 6, 11, 16, \ldots, 91, 96$.

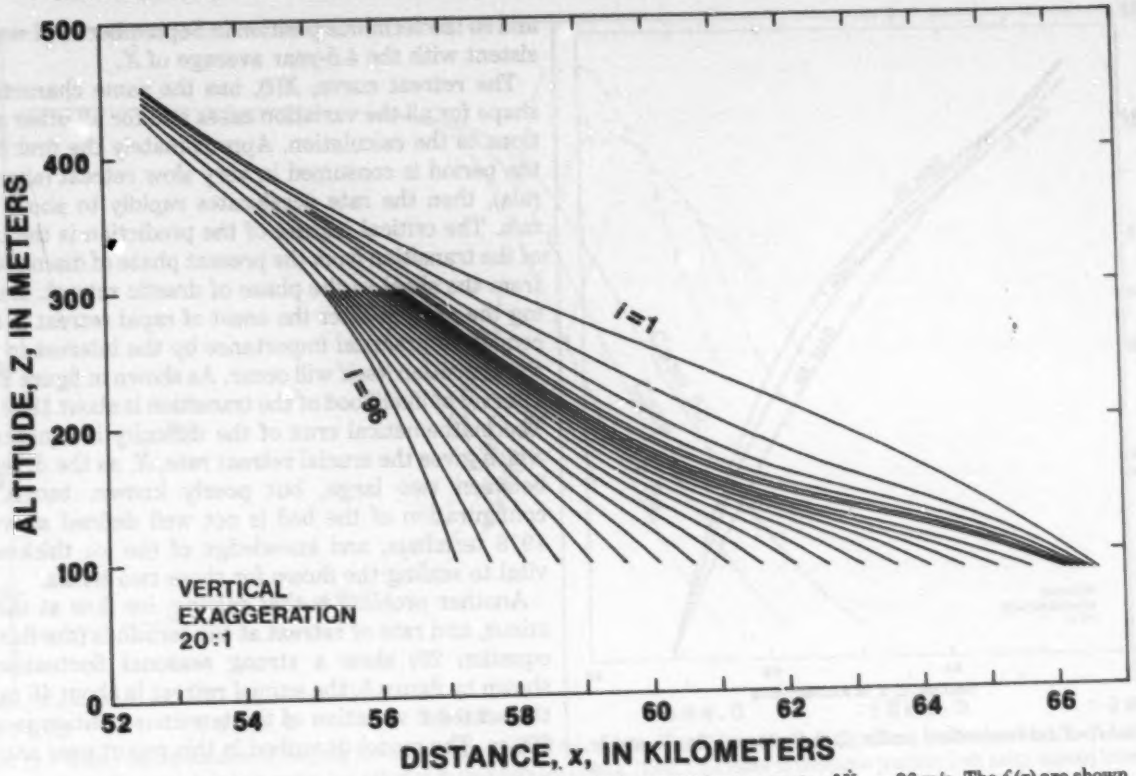

FIGURE 15.–Longitudinal profiles for case 7a that are compatible with an initial retreat rate of $\dot{X}_1 = -36$ m/a. The $f_i(x)$ are shown for $i = 1, 2, 3, 4, 5, 6, 11, 16, \ldots, 91, 96$.

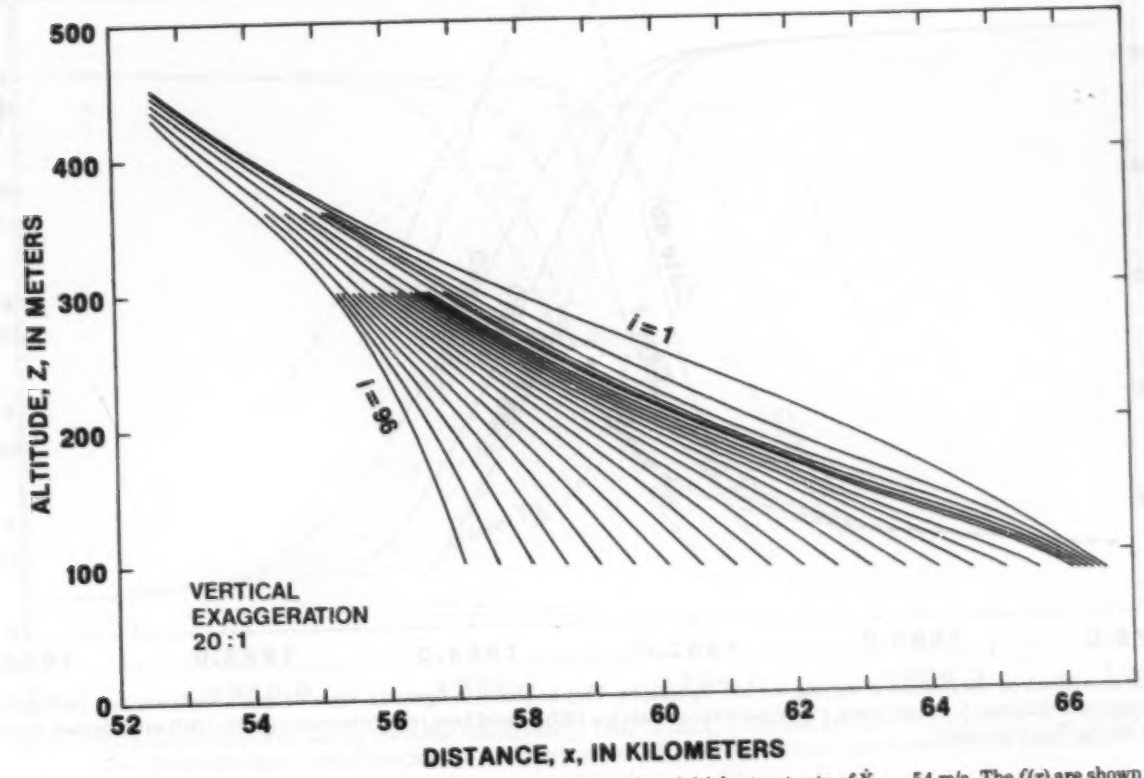

FIGURE 16.–Longitudinal profiles for base 7b that are compatible with an initial retreat rate of $\dot{X}_1 = -54$ m/a. The $f_i(x)$ are shown for $i = 1, 2, 3, 4, 5, 6, 11, 16, \ldots, 91, 96$.

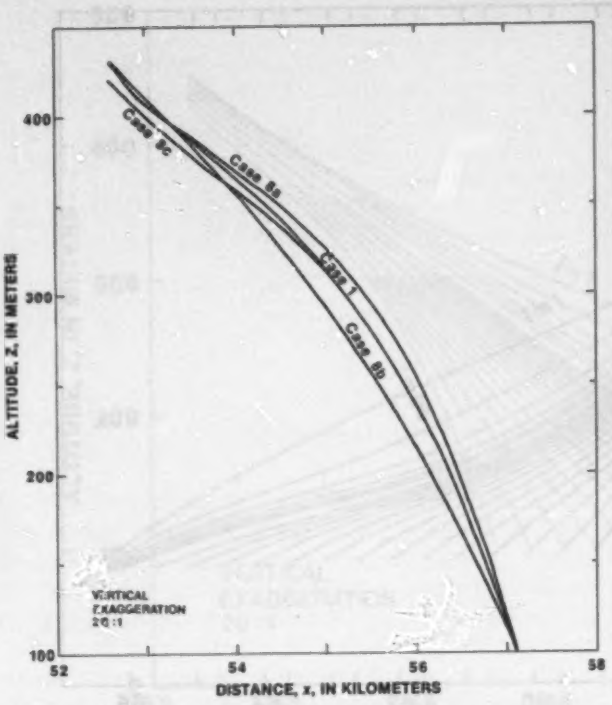

FIGURE 17. – Final longitudinal profile, $f_{ss}(x)$, for cases 1, 8a, 8b, and 8c.

and so the terminus position in September 1981 was consistent with the 4.5-year average of $\dot{X}$.

The retreat curve, $X(t)$, has the same characteristic shape for all the variation cases and for all other alterations to the calculation. Approximately the first half of the period is consumed in very slow retreat (about 100 m/a), then the rate accelerates rapidly to about 3,000 m/a. The critical feature of the prediction is the timing of the transition from the present phase of disconnection from the shoal to the phase of drastic retreat. Describing the process after the onset of rapid retreat is transcended in practical importance by the interest in when the transition itself will occur. As shown in figure 22, the interval of likelihood of the transition is about 1982 ± 0.9. The mathematical crux of the difficulty is equation 20, which gives the crucial retreat rate, $\dot{X}$, as the difference between two large, but poorly known, terms. The configuration of the bed is not well defined above the 1978 terminus, and knowledge of the ice thickness is vital to scaling the fluxes for those two terms.

Another problem is that calving, ice flow at the terminus, and rate of retreat at the terminus (the fluxes in equation 20) show a strong seasonal fluctuation; as shown by figure 5, the annual retreat is about 45 m, and the seasonal variation of the terminus position is about 300 m. The model described in this report uses annually

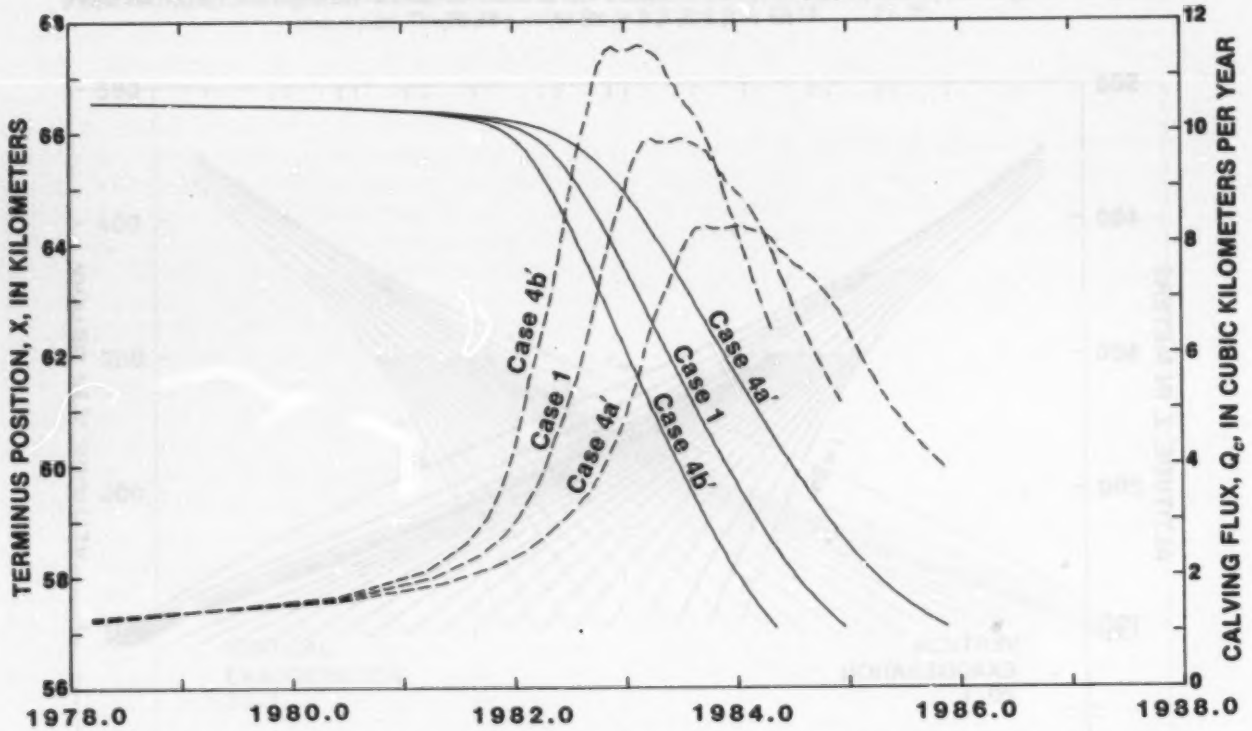

FIGURE 18. – Effect on the solution of varying the bed topography, $U(x)$, as shown in figure 11. Case 4a′ uses a shallower bed, and case 4b′, a deeper bed, than case 1; in both cases, c is adjusted to maintain $t_2 = 1980.4$. Solid lines refer to terminus position (left axis); dashed lines refer to calving flux (right axis).

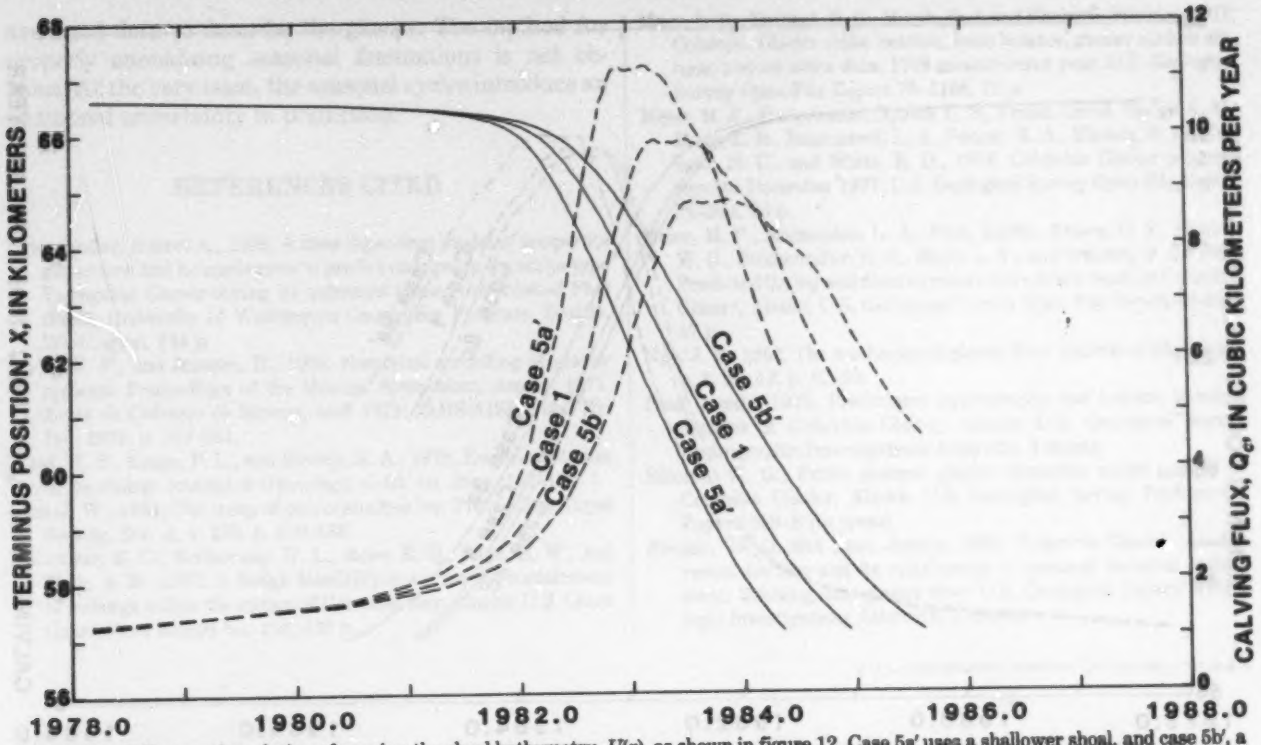

FIGURE 19.—Effect on the solution of varying the shoal bathymetry, $U(x)$, as shown in figure 12. Case 5a' uses a shallower shoal, and case 5b', a deeper shoal, than case 1; in both cases, c is adjusted to maintain $t_2 = 1980.4$. Solid lines refer to terminus position (left axis); dashed lines refer to calving flux (right axis).

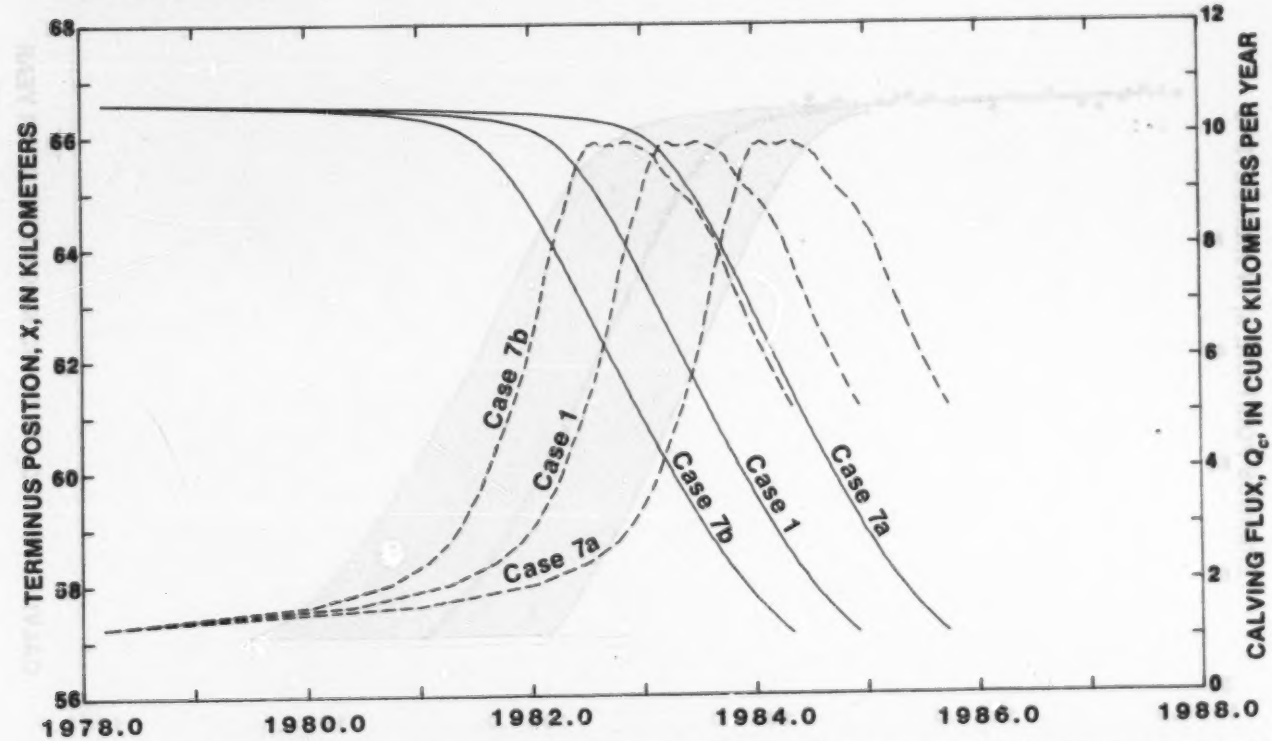

FIGURE 20.—Effect on the solution of varying the initial retreat rate $\dot{X}_1$. Case 7a has $\dot{X}_1 = -36$ m/a, and case 7b has $\dot{X}_1 = -54$ m/a, compared with $\dot{X}_1 = -45$ m/a for case 1. Solid lines refer to terminus position (left axis); dashed lines refer to calving flux (right axis).

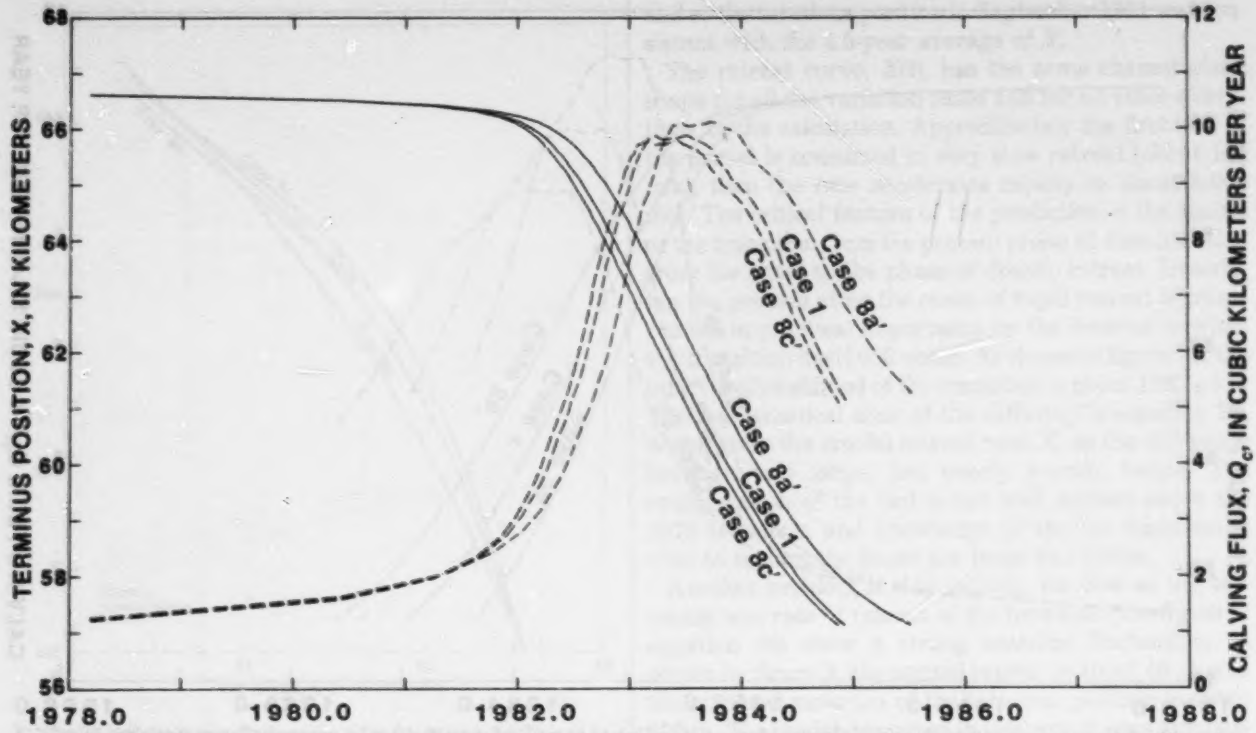

FIGURE 21.—Effect on the solution of varying the final longitudinal profile, $f_\infty(x)$, as shown in figure 17. Case 8a′ uses a steepened profile and an increased discharge, $Q_{s\infty}$, and case 8c′, a lower altitude, $Z_{s\infty}$, than case 1; in both cases, c is adjusted to maintain $t_3 = 1980.4$. Solid lines refer to terminus position (left axis); dashed lines refer to calving flux (right axis).

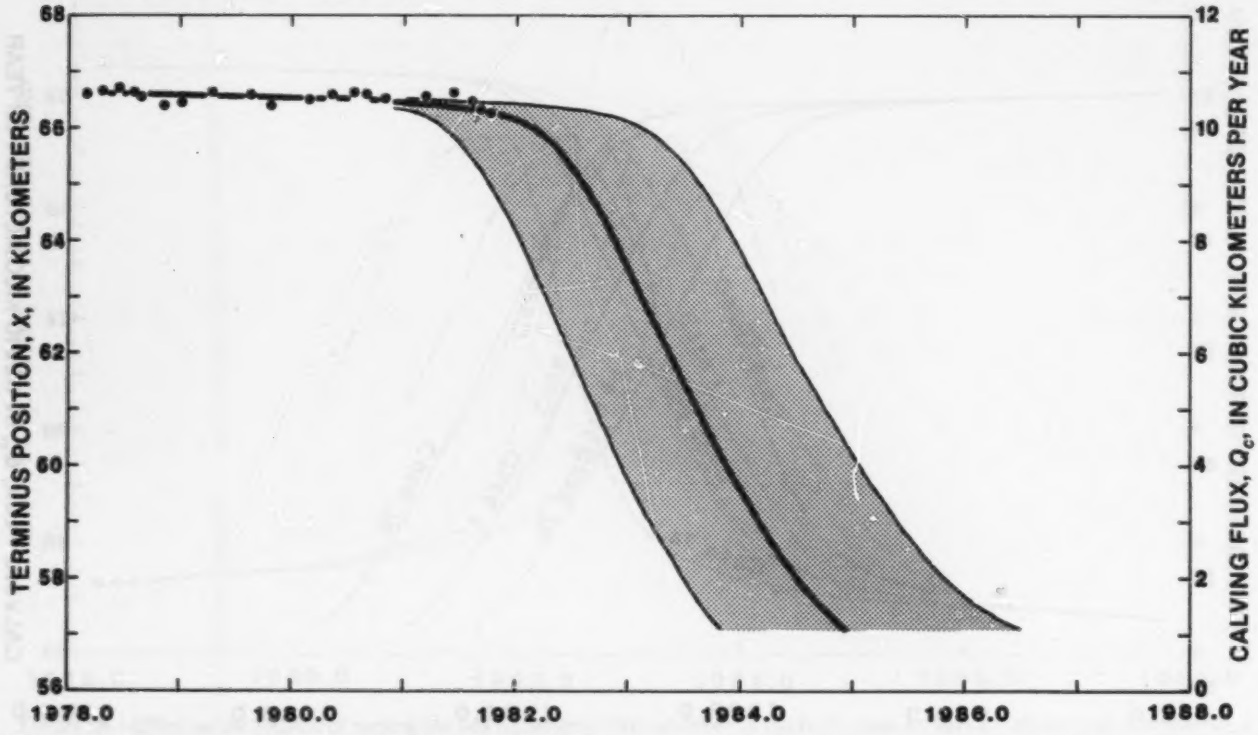

FIGURE 22.—Resultant summation of the individual errors that may be present in the data used to describe Columbia Glacier. The likely early retreat, $X_E(t)$, and the likely late retreat, $X_L(t)$, are shown, along with $X(t)$ for case 1. The probability assigned to $X_E(t)$ and $X_L(t)$ is the same as that ascribed to the variations of the data in cases 2–8. Observed values of $X(t)$ are indicated by dots (see fig. 5).

averaged data to describe the glacier. The method for properly annualizing seasonal fluctuations is not obvious. At the very least, the seasonal cycles introduce an additional uncertainty in prediction.

REFERENCES CITED

Bindschadler, Robert A., 1978, A time-dependent model of temperate glacer flow and its application to predict changes in the surge-type Variegated Glacier during its quiescent phase: Unpublished PhD thesis, University of Washington Geophysics Program, Seattle, Washington, 244 p.

Budd, W. F., and Jenssen, D., 1975, Numerical modelling of glacier systems: Proceedings of the Moscow Symposium, August 1971; Actes du Colloque de Moscou, aout 1971: IAHS-AISH Publ. No. 104, 1975, p. 257–291.

Budd, W. F., Keage, P. L., and Blundy, N. A., 1979, Empirical studies of ice sliding: Journal of Glaciology, v. 23, no. 89, p. 157–170.

Glen, J. W., 1954, The creep of polycrystalline ice: Proceedings Royal Society, Ser. A, v. 228, p. 519–538.

Kollmeyer, R. C., Motherway, D. L., Robe, R. Q., Platz, B. W., and Shah, A. M., 1977, A design feasibility study for the containment of icebergs within the waters of Columbia Bay, Alaska: U.S. Coast Guard Final Report No. 128, 135 p.

Mayo, L. R., Trabant, D. C., March, Rod, and Haeberli, Wilfried, 1979, Columbia Glacier stake location, mass balance, glacier surface altitude, and ice radar data, 1978 measurement year: U.S. Geological Survey Open-File Report 79–1168, 72 p.

Meier, M. F., Post, Austin, Brown, C. S., Frank, David, Hodge, S. M., Mayo, L. R., Rasmussen, L. A., Senear, E. A., Sikonia, W. G., Trabant, D. C., and Watts, R. D., 1978, Columbia Glacier progress report–December 1977: U.S. Geological Survey Open-File Report 78–264, 56 p.

Meier, M. F., Rasmussen, L. A., Post, Austin, Brown, C. S., Sikonia, W. G., Bindschadler, R. A., Mayo, L. R., and Trabant, D. C., 1980, Predicted timing and disintegration of the lower reach of Columbia Glacier, Alaska: U.S. Geological Survey Open-File Report 80–582, 47 p.

Nye, J. F., 1952, The mechanics of glacier flow: Journal of Glaciology, v. 2, no. 12, p. 82–93.

Post, Austin, 1975, Preliminary hydrography and historic terminal changes of Columbia Glacier, Alaska: U.S. Geological Survey Hydrographic Investigations Atlas 559, 3 sheets.

Sikonia, W. G., Finite element glacier dynamics model applied to Columbia Glacier, Alaska: U.S. Geological Survey Professional Paper 1258–B [in press].

Sikonia, W. G. and Post, Austin, 1980, Columbia Glacier, Alaska: recent ice loss and its relationship to seasonal terminal embayment, thinning, and glacier flow: U.S. Geological Survey Hydrologic Investigations Atlas 619, 3 sheets.

☆U.S. GOVERNMENT PRINTING OFFICE: 1982—361-614/4

DEPARTMENT OF THE INTERIOR
U.S.
March 3, 1849